J. Fluid Mech. (2012), *vol.* 690, *pp.* 474–498. © Cambridge University Press 2011
doi:10.1017/jfm.2011.452

A study of two-fluid model equations

K. Ueyama†

Department of Environmental and Energy Chemistry, Kogakuin University, 1-24-2 Nishishinjyuku, Shinjyuku, Tokyo 163-8677, Japan

(Received 26 May 2010; revised 23 September 2011; accepted 14 October 2011; first published online 25 November 2011)

A theoretical study of the interaction term in the two-fluid model equations is presented. The relevant Navier–Stokes equation is volume-integrated in a control volume fixed in a field of dispersed two-phase flow; then it is time-integrated. An expression for the interaction term is obtained in the limit of infinitesimal control volume, which rigorously fits to the two-fluid model equation based on time averaging. The interaction term is then analysed for dispersed two-phase flow with homogeneous particle size. The mathematical expression of the resulting interaction term clearly shows its property, which has been overlooked for more than 40 years. It can be decomposed into the conventional interaction term and an additional 'virtual force' term. The virtual force term is evaluated approximately for two types of dispersed multiphase flow in order to demonstrate its effectiveness. The first is solid–liquid dispersed two-phase flow with spherical solid particles undergoing creeping flow, and the second is gas–liquid dispersed two-phase flow with large bubbles in a highly turbulent flow field. For solid spherical particles in a homogeneous creeping flow, the term vanishes, as was found numerically by Ten Cate and Sundaresan (*Intl J. Multiphase Flow*, vol. 32, 2006, pp. 106–131), although the term could be significant for a flow field with velocity gradient. For large bubbles in bubble columns in a recirculating turbulent flow regime, the term is significant. The two-fluid model equations are corrected by the introduction of these virtual force terms, which in some circumstances are important in simulating the macroscopic properties of dispersed two-phase flow with spatial variations.

Key words: computational methods, multiphase flow, Navier–Stokes equations

1. Introduction

Two-fluid model equations have been widely used to calculate the macroscopic properties of multiphase flow across time and space, in which the averaged values of the physical quantities specifying each phase, such as velocity, pressure and local hold up, are represented by continuous distributions in space by means of a suitable averaging process. Ishii & Hibiki (2006) classified three distinct types of averaging: the Eulerian average, the Lagrangian average and the Boltzmann statistical average. No matter how the averaging is done, the two-fluid model equations relate the spatial distributions of averaged physical quantities of continuous or dispersed phases to the interaction force at the interface. There is also a strong demand that the interaction

† Email address for correspondence: ueyama@cc.kogakuin.ac.jp

https://doi.org/10.1017/jfm.2011.452 Published online by Cambridge University Press

term in the two-fluid model equation is to be given in terms of the forces acting on a particle, such as the drag force, the lift force and the virtual mass force, so that we can use the accumulated knowledge on the forces.

The volume-averaged two-fluid model equations were first proposed independently in the same year by Anderson & Jackson (1967), Whitaker (1967) and Slattery (1967), based on the mathematically rigorous relation between the space derivative of the volume average and the volume average of the space derivative.

Anderson & Jackson (1967) proposed a theory for volume averaging of the spatially distributed physical quantities by using a weight function, and gave a definition for the radius of the weight function. By applying the volume averaging theory to the equation of continuity, the Navier–Stokes equation and the equation of motion for a particle, they obtained the equations of continuity for the fluid and particle phases, the two-fluid model equation for the fluid phase and the equation of motion for a particle, respectively. The interaction term in the two-fluid model equation was given as a product of the number density of the particle phase and the force acting on a particle surface, mainly under the assumption that the radius of the weight function is between the particle size and the size of the macroscopic distribution. Then, the accumulated knowledge on the force acting on a particle could have been used.

Whitaker (1967) applied mathematically rigorous relations between the space derivative of the volume average and the volume average of the space derivative to the equation of continuity, the diffusion equation and the Navier–Stokes equation for the fluid phase, and obtained basic equations for the flow through porous media. In the two-fluid model equation that he obtained, the interaction term was given as the force acting on the fluid phase at the surface of the porous media.

Slattery (1967) also discussed the flow in porous media, focusing on the flow of viscoelastic fluids. He took almost the same route as Whitaker, and obtained the two-fluid model equation for the fluid phase. Slattery showed that Darcy's law was seen from the interaction term obtained in the two-fluid model equation.

In considering the interaction term, the theory of volume averaging has been refined by Jackson (2000), and the interaction term was given rigorously as the sum of the conventional interaction term, which is the product of the number density of the particle phase and the force acting on a particle surface, and a further supplementary term that is related to the spatial gradient of the local holdup. The supplementary term is not readily interpreted in terms of the force acting on the particle, because of its complicated mathematical form.

In the two-fluid model equation based on time averaging, the interaction term has been given as a sum of impacts due to the appearance of surfaces at the point of interest (Ishii 1975; Ueyama & Miyauchi 1976). The interaction term rigorously fits to the time-averaged two-fluid model equations, in which the terms can be defined at any point in space. The relation between the impact term and the analysis of the force acting on a particle was not intuitive, however. This is presumably why most papers have worked with the volume-averaged equations.

Practically and scientifically important results of the statistical average have been found. Batchelor (1970) applied the theory of ensemble averaging to fluid–particle two-phase flow, and showed that the apparent viscosity influencing the motion of a particle is given by the Einstein equation. Hinch (1977) made clear the hierarchy aspect of the ensemble average for the effect of the void fraction of the particle phase on the apparent viscosity. Both approaches focus mainly on the effect of the volume fraction of the particle phase on the apparent viscosity; the relation between the interaction term and the force acting on a particle was not seen in the resulting

https://doi.org/10.1017/jfm.2011.452 Published online by Cambridge University Press

two-fluid model equation, however. Zhang & Prosperetti (1994) took the ensemble mean for the fluid phase and for the particle phase by introducing a phase function. The ensemble mean of a space derivative and the space derivative of an ensemble mean were distinguished. However, the relation between the interaction term they derived and the force acting on a particle was not intuitive, just like the impact term in the two-fluid model equation based on the time averaging, and the effect of the particle size was not explicit in the resulting two-fluid model equation, because of the small-particle approximation involved. Zhang and Prosperetti introduced a stress term arising from the fluctuating motion of the particles. The stress term is related to the gradient of the local volume fraction of the particle phase. This term may be an important part of the dispersion force (Lahey, Bertodano & Jones 1993; de Bertodano, Lahey & Jones 1994), to which attention has been paid in the context of numerical experiments of multiphase flow (Hibiki & Ishii 2007; Tabib, Roy & Joshi 2008).

Aside from the three categories of averaging, Drew (1983) showed a common feature of the averaging process (time average, volume average and ensemble average) by introducing the notions of generalized function and test function. However, this approach was not capable of extending the previous work based on volume averaging, time averaging or statistical averaging.

Now, it can be concluded that the reason why the control volume is restricted to be between the particle size and the scale of macroscopic variation, even in recent textbooks such as Brennen (2005) and Kolev (2007), is that the interaction term in the two-fluid model equation obtained theoretically cannot be interpreted solely in terms of a force acting on a particle centred at the point of reference.

The supplementary term introduced by Jackson (2000) and the stress term introduced by Zhang & Prosperetti (1994) are both related to the spatial gradient of the local holdup of the dispersed phase. Jackson's term should not be included in an equation of motion for a particle, because the term is introduced into the two-fluid model equation for the fluid phase as the gap between the rigorous interaction term and the conventional interaction term. The term of Zhang and Prosperetti reflects the effect of fluctuating motion, which is a real physical phenomenon known as the Reynolds stress, and appears in both the equation of motion for a particle and the two-fluid model equation for the fluid phase. It is clear that there are two kinds of term relating to the local holdup gradient that are to be included in the two-fluid model equation. One is a supplementary term that is the gap between the rigorous interaction term in the two-fluid model equation and the conventional interaction term; the other is a term related to the Reynolds stress. The term relating to the local gradient of holdup has been studied numerically. Hibiki & Ishii (2007), Lahey *et al.* (1993), de Bertodano *et al.* (1994) and Tabib *et al.* (2008) demonstrated the importance of this term, although Ten Cate & Sundaresan (2006) reported that the term involving the spatial gradient of the local holdup does not influence flow through a particle-packed bed with a spatial gradient of packing, based on numerical simulations using the lattice–Boltzmann method. The physical meaning and the effectiveness of the term related to the gradient of the local holdup remain unclear.

The main purpose of this work is to reveal the intrinsic property of the interaction term in the two-fluid model equation, which affords an interpretation of the gap between the rigorous interaction term and the conventional interaction term in terms of a force acting on a particle surface with its centre at the point of interest. The theory shows clearly how to fit the analysis of the force acting on a particle to the interaction term in the two-fluid model equations, and suggests further research by highlighting some issues remaining over the relation between the interaction term and the force

https://doi.org/10.1017/jfm.2011.452 Published online by Cambridge University Press

acting on a particle. The physical meanings of the terms in the equation of motion for a particle in dispersed two-phase flow are also discussed, giving clear physical interpretations of the various forces acting on the particle.

The paper is organized as follows. In § 2, the relevant Navier–Stokes equation is volume-integrated over a control volume fixed in a dispersed two-phase flow field, and then time-integrated. An expression for the interaction term is obtained in the limit of infinitesimal control volume; this term rigorously fits to the interaction term in the two-fluid model equation based on time averaging. In §§ 3.1, 3.2 and 3.3, the mathematical expression for the interaction term is derived for dispersed two-phase flow with a uniform size of spherical particles. The resulting interaction term differs from the conventional interaction term through its 'inside-out' property (see § 3.3), which will be explained in detail below. (The 'inside-out' expression is generalized to non-spherical particles in Appendix D of the supplementary material, available at journals.cambridge.org/flm.) In § 3.4, the interaction term with the 'inside-out' property is resolved into the conventional interaction term plus virtual force terms that make up the discrepancy between the 'inside-out' interaction term and the conventional interaction term; this is achieved using a Taylor expansion to shift the point where the physical quantities are assigned. The virtual force term thus introduced is not a model to be evaluated in various ways, but is an inevitable outcome of the rigorous interaction term. In § 4, an equation of motion for a particle in dispersed two-phase flow is derived, with a clear physical interpretation of each term in the equation. A relation between the time-averaged moving velocity of a particle and the time-averaged velocity of the dispersed phase has been derived, which shows that the two averaged velocities are to be distinguished when neither the time-averaged moving velocity of particles nor the local holdup are homogeneous in space. The buoyancy term has been picked out of the equation of motion for a particle by using the relevant Navier–Stokes equation, and the reference density in the buoyancy term has been shown to be the mean density of the surrounding two-phase mixture. In § 5, the value of the virtual force term is evaluated approximately for creeping flow around spherical solid particles and for gas–liquid dispersed flow with bubbles in a category of spherical cap bubbles in a highly turbulent flow, to illustrate the effectiveness of the virtual force term and to demonstrate the urgent demand for research aimed at the reliable usage of the virtual force term. The two-fluid model equation with the virtual force term is described in the final section, § 6, together with a brief discussion of each term in the equation.

2. Interaction term in two-fluid model equation

For dispersed two-phase flow, an equation is obtained by integrating the relevant Navier–Stokes equation for flow of the continuous phase over the entire volume of the continuous phase in a control volume, V, as follows:

$$\int_V H_c \left\{ \frac{\partial}{\partial t}(\rho_c \boldsymbol{u}_c) + \boldsymbol{\nabla} \cdot (\rho_c \boldsymbol{u}_c \boldsymbol{u}_c) - \rho_c \boldsymbol{g} \right\} \mathrm{d}V + \int_S H_c \{\boldsymbol{n} \cdot (P_c \boldsymbol{I} + \boldsymbol{\tau}_c)\} \, \mathrm{d}S = -\boldsymbol{F}^V_{R,S}. \quad (2.1)$$

Here, ρ_c, $\boldsymbol{u}_c$, P_c and $\boldsymbol{\tau}_c$, respectively, denote the density, velocity vector, static pressure and shear stress tensor of the continuous phase. The symbols S, $\boldsymbol{I}$ and $\boldsymbol{n}$ refer to the surface of the control volume, unit tensor and unit normal vector outwardly directed on S. Also, H_c denotes a step function of position, taking value unity when the position is occupied by the continuous phase and zero when the position is occupied by the dispersed phase. The term $\boldsymbol{F}^V_{R,S}$ on the right-hand side is the sum of forces

https://doi.org/10.1017/jfm.2011.452 Published online by Cambridge University Press

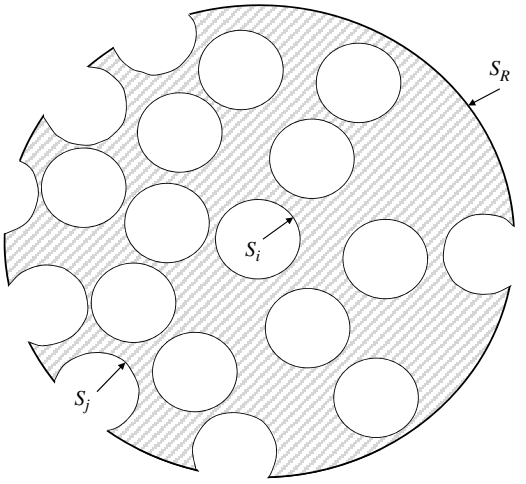


FIGURE 1. Particle surfaces in a control volume.

acting on particle surfaces in the control volume, and is given by

$$\boldsymbol{F}^V_{R,S} = \sum_i \oint_{S_i} \{\boldsymbol{m} \cdot (P_c \boldsymbol{I} + \boldsymbol{\tau}_c)\}\, \mathrm{d}S + \sum_j \int_{S_j} \{\boldsymbol{m} \cdot (P_c \boldsymbol{I} + \boldsymbol{\tau}_c)\}\, \mathrm{d}S, \tag{2.2}$$

where S_i and S_j are particle surfaces within the control volume: S_i denotes the surface of the particle i that is entirely within the control volume, and S_j is the surface of the particle j to be partly cut by the surface bounding the control volume. The notation $\sum_i$ and $\sum_j$ refers to summation over each category of particle. In (2.2), $\boldsymbol{m}$ is a unit normal vector directed inwards on each category of particle surface. Since the theory to be developed here is assuming the dispersed two-phase flow in general, the terminology 'particle' does not solely mean solid particle, but also represents bubble or liquid drop.

In the derivation of the volume-averaged two-fluid model equations, the terms on the left-hand side of (2.1) are transformed to time and space derivative terms of averaged physical quantities (Anderson & Jackson 1967; Whitaker 1967), and the right-hand side of (2.1) is given as the conventional interaction term under the restriction of the size of the control volume (Anderson & Jackson 1967; Kolev 2007). Since no restriction is assumed for the transformation of the left-hand side, let us consider the right-hand side for a control volume having size comparable to the scale of macroscopic variations.

For the case shown in figure 1, where particles are rich on the left-hand side, it is easily seen that the first term on the right-hand side of (2.2) is represented by a force acting on a particle centred in the left-hand side of the control volume, and that the force acting on the right-hand side hemisphere of a particle is dominant in the second term on the right-hand side of (2.2). If we take a control volume smaller than a particle size, the first term on the right-hand side of (2.2) disappears, but the effect of imbalance in the forces acting on the right- and left-hand side hemispheres of the particle still remains. It is obvious that the effect of the spatial distribution itself depends on the size of the control volume. The forces acting on hemispherical surfaces of a particle are important in the foundation of this work.

https://doi.org/10.1017/jfm.2011.452 Published online by Cambridge University Press

Let us take a time average of (2.1) over a duration Λ from $t-(\Lambda/2)$ to $t+(\Lambda/2)$, in order to consider the effect of the spatial distribution of the flow field. Since the volume V and surface S are independent of time, we obtain

$$\overline{\boldsymbol{F}_{R,S}^{V}}^{\Lambda} = -\int_V \left[\frac{\partial}{\partial t}\{(1-\epsilon)\overline{\rho_c \boldsymbol{u}_c}^{c}\} + \boldsymbol{\nabla}\cdot\{(1-\epsilon)\overline{\rho_c \boldsymbol{u}_c \boldsymbol{u}_c}^{c}\} - (1-\epsilon)\overline{\rho_c}^{c}\boldsymbol{g}\right] \mathrm{d}V$$
$$- \int_S \{(1-\epsilon)\boldsymbol{n}\cdot(\overline{P_c}^{c}\boldsymbol{I} + \overline{\boldsymbol{\tau}_c}^{c})\}\,\mathrm{d}S. \tag{2.3}$$

In deriving (2.3) the following equation has been used:

$$\frac{1}{\Lambda}\int_{t-(\Lambda/2)}^{t+(\Lambda/2)} \left[H_c \frac{\partial}{\partial t}(\rho_c \boldsymbol{u}_c) + \boldsymbol{\nabla}\cdot(\rho_c \boldsymbol{u}_c \boldsymbol{u}_c)\right] \mathrm{d}t$$
$$= \frac{\partial}{\partial t}\{(1-\epsilon)\overline{\rho_c \boldsymbol{u}_c}^{c}\} + \boldsymbol{\nabla}\cdot\{(1-\epsilon)\overline{\rho_c \boldsymbol{u}_c \boldsymbol{u}_c}^{c}\}. \tag{2.4}$$

Equation (2.4) is derived in Appendix A of the supplementary material. Here, $\overline{q}^{\Lambda}$ and $\overline{q}^{c}$ denote time-averaged values of a physical quantity q for the total duration of averaging Λ, and total duration for which the continuous phase covers the point of interest, Λ_c, as defined by the following equations:

$$\overline{q}^{\Lambda} = \frac{1}{\Lambda}\int_{t-(\Lambda/2)}^{t+(\Lambda/2)} q(\boldsymbol{X}, t)\,\mathrm{d}t, \tag{2.5}$$

$$\overline{q}^{c}(\boldsymbol{X}, t) = \frac{1}{\Lambda_c}\int_{\Lambda_c} q(\boldsymbol{X}, t)\,\mathrm{d}t. \tag{2.6}$$

Here, $\boldsymbol{X}$ is a position vector and $\int_{\Lambda_c} q(\boldsymbol{X}, t)\,\mathrm{d}t$ is the time integral of $q(\boldsymbol{X}, t)$ over the duration for which the point $\boldsymbol{X}$ is covered by the continuous phase. The parameter ϵ in (2.3) is the local holdup of the dispersed phase, defined as the ratio of Λ_d to the total time averaging duration, Λ, where Λ_d is the total time duration during which the point of interest is occupied by the dispersed phase. Consequently, $(1-\epsilon)$ in (2.3) is the local holdup of the continuous phase. The following relations hold, where suffices c and d refer to the continuous and dispersed phases:

$$\Lambda = \Lambda_c + \Lambda_d, \tag{2.7}$$

$$\epsilon = \frac{\Lambda_d}{\Lambda}, \tag{2.8}$$

$$\overline{q_c}^{\Lambda}(\boldsymbol{X}, t) = \frac{1}{\Lambda}\int_{t-(\Lambda/2)}^{t+(\Lambda/2)} H_c q_c(\boldsymbol{X}, t)\,\mathrm{d}t = \frac{\Lambda_c}{\Lambda}\frac{1}{\Lambda_c}\int_{\Lambda_c} q_c(\boldsymbol{X}, t)\,\mathrm{d}t$$
$$= (1-\epsilon)\overline{q_c}^{c}(\boldsymbol{X}, t), \tag{2.9}$$

$$\overline{q_d}^{\Lambda}(\boldsymbol{X}, t) = \epsilon\,\overline{q_d}^{d}(\boldsymbol{X}, t). \tag{2.10}$$

The second term on the right-hand side of (2.3) can be transformed to a volume integral using Gauss' theorem, so that, from (2.3),

$$\overline{\boldsymbol{F}_{R,S}^{V}}^{\Lambda} = -\int_V \left[\frac{\partial}{\partial t}\{(1-\epsilon)\overline{\rho_c \boldsymbol{u}_c}^{c}\} + \boldsymbol{\nabla}\cdot\{(1-\epsilon)\overline{\rho_c \boldsymbol{u}_c \boldsymbol{u}_c}^{c}\} - (1-\epsilon)\overline{\rho_c}\boldsymbol{g}\right.$$
$$\left. + \boldsymbol{\nabla}\cdot\left[(1-\epsilon)\{\overline{P_c}^{c}\boldsymbol{I} + \overline{\boldsymbol{\tau}_c}^{c}\}\right]\right] \mathrm{d}V. \tag{2.11}$$

https://doi.org/10.1017/jfm.2011.452 Published online by Cambridge University Press

In general, for a function of position $G(\boldsymbol{X})$, when volume V converges to a point $\boldsymbol{X}_0$, we have

$$\lim_{V\to\boldsymbol{X}_0}\left\{\frac{1}{V}\int_V G(\boldsymbol{X})\,\mathrm{d}V\right\}=G(\boldsymbol{X}_0). \tag{2.12}$$

The limit $\lim_{V\to\boldsymbol{X}_0}$ is the value when the control volume converges to a point $\boldsymbol{X}_0$.

From (2.11) and (2.12), it follows that

$$\lim_{V\to\boldsymbol{X}_0}\frac{1}{V}\overline{\boldsymbol{F}_{R,S}^{V}}^{\Lambda}=-\frac{\partial}{\partial t}\{(1-\epsilon)\overline{\rho_c\boldsymbol{u}_c}^{c}\}-\boldsymbol{\nabla}\cdot\{(1-\epsilon)\overline{\rho_c\boldsymbol{u}_c\boldsymbol{u}_c}^{c}\}+(1-\epsilon)\overline{\rho_c}^{c}\boldsymbol{g}$$
$$-\boldsymbol{\nabla}\cdot[(1-\epsilon)\{\overline{P_c}^{c}\boldsymbol{I}+\overline{\boldsymbol{\tau}_c}^{c}\}]. \tag{2.13}$$

The terms on the right-hand side are specified at a point $\boldsymbol{X}_0$ to which the control volume converges. The left-hand side of (2.13) gives the interaction term without any restriction on the averaging. Equation (2.13) shows that the interaction term in the two-fluid model equations based on time averaging is the time-averaged force acting on particle surfaces in an infinitesimal size of control volume, that is, $\lim_{V\to\boldsymbol{X}_0}(1/V)\overline{\boldsymbol{F}_{R,S}^{V}}^{\Lambda}$. Remembering the discussion above, the force acting on subsurfaces of a particle cut by a plane perpendicular to the spatial gradient of the local holdup should play an important role in the interpretation of $\lim_{V\to\boldsymbol{X}_0}(1/V)\overline{\boldsymbol{F}_{R,S}^{V}}^{\Lambda}$.

We next analyse the value of $\overline{\boldsymbol{F}_{R,S}^{V}}^{\Lambda}=(1/\Lambda)\int_{t-(\Lambda/2)}^{t+(\Lambda/2)}\boldsymbol{F}_{R,S}^{V}\,\mathrm{d}t$ for a control volume much smaller than a particle size, and take the limit value of $(1/V)\overline{\boldsymbol{F}_{R,S}^{V}}^{\Lambda}$ for $V\to\boldsymbol{X}_0$.

3. Interaction term resolved for dispersed two-phase flow with homogeneous spherical drop size

This section sets out to obtain the interaction force per unit volume at a fixed point in space, suitable for use in the two-fluid model equations. Since the analysis concentrates on intrinsic properties of the interaction term, homogeneous size of spherical particles is assumed, and also the absence of mass transfer across the interface and no surface tension effects.

3.1. *Basic concepts and notation system*

A spherical coordinate system is used to express the value of a physical quantity q around a point $\boldsymbol{X}$ in a space, as $q(\boldsymbol{X}:r,\theta,\phi,t)$, where $\boldsymbol{X}$ is the origin of the spherical coordinate system and coordinates (r,θ,ϕ) are defined in a right-hand Cartesian coordinate system, as shown in figure 2. The same Cartesian coordinate system is used for a spherical coordinate system around each point under consideration; hence the unit normal vector along the r axis with the same angular coordinates is common to all spherical coordinate systems. Where two spherical coordinate systems about two points $\boldsymbol{X}_0$ and $\boldsymbol{X}'$ are used simultaneously, the notations $(\boldsymbol{X}_0:r,\theta,\phi)$ and $(\boldsymbol{X}':r',\theta',\phi')$ are used, whereas the Cartesian coordinate system is common. The notation $\overline{q}^{\Lambda}(\boldsymbol{X}:r,\theta,\phi)$ is used to express the time-averaged value of a physical quantity q, at the point $(\boldsymbol{X}:r,\theta,\phi)$ over the duration Λ. Although the value of a time-averaged physical quantity itself varies with time as defined by (2.5) or (2.6), we omit time t from the expression of time-averaged physical quantities henceforth for the sake of simple expression.

The local holdup of the dispersed phase at a fixed point $\boldsymbol{X}$ in a space, $\epsilon(\boldsymbol{X})$, is defined as the ratio of the duration $\Lambda_d(\boldsymbol{X})$ for which the point $\boldsymbol{X}$ is covered by the

https://doi.org/10.1017/jfm.2011.452 Published online by Cambridge University Press

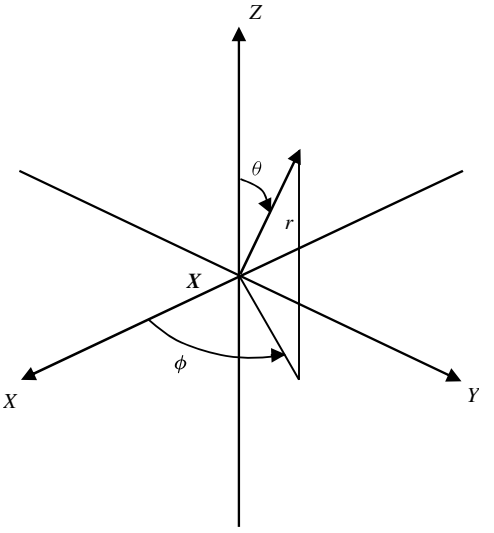


FIGURE 2. Spherical coordinate system.

dispersed phase, to the total time averaging interval Λ:

$$\epsilon(\boldsymbol{X}) = \frac{\Lambda_d(\boldsymbol{X})}{\Lambda}. \tag{3.1}$$

For a control volume V smaller than a particle, we can define the duration λ_R^V for which the centre of particles with radius R is observed in V throughout a total duration Λ. It is also possible to define a duration $\lambda_R(\boldsymbol{X})$ in which the centre of a particle with radius R is in unit volume assigned at point $\boldsymbol{X}$,

$$\lambda_R(\boldsymbol{X}) = \lim_{V \to \boldsymbol{X}} \frac{\lambda_R^V}{V}. \tag{3.2}$$

The values of λ_R^V and V approach zero for $V \to \boldsymbol{X}$, but we expect a finite value for λ_R, as with a molar concentration assigned at a point in a space. It should be noted here that λ_R is defined as time length per unit volume assigned at a point in space, and hence the dimension of λ_R is time divided by volume.

Since the centre of the volume V can be chosen at any point in space, the value of λ_R is also given at any point in space. The value of Λ_d at a fixed point $\boldsymbol{X}_0$ is now given by

$$\Lambda_d(\boldsymbol{X}_0) = \int_0^{\pi} \mathrm{d}\theta \int_0^{2\pi} \mathrm{d}\phi \left[\sin\theta \int_0^R r^2 \lambda_R(\boldsymbol{X}_0 : r, \theta, \phi)\, \mathrm{d}r \right]. \tag{3.3}$$

On the right-hand side of (3.3), the integrand for the angular integration is shown in square brackets; this notation will be used henceforth for the angular integration.

3.2. *The conventional interaction term*

The force acting on a particle surface with its centre at point $\boldsymbol{X}_0$ is given by

$$\boldsymbol{f}_p(\boldsymbol{X}_0, t) = -\int_0^{\theta} \mathrm{d}\theta \int_0^{2\pi} \mathrm{d}\phi \left[\sin\theta\, R^2 \boldsymbol{n}(\theta, \phi) \cdot \boldsymbol{T}_c(\boldsymbol{X}_0 : R, \theta, \phi, t) \right]. \tag{3.4}$$

https://doi.org/10.1017/jfm.2011.452 Published online by Cambridge University Press

Here, $\boldsymbol{n}(\theta,\phi)$ is a unit vector along the r axis in the spherical coordinate system $\{\boldsymbol{X}_0 : r,\theta,\phi\}$ and $\boldsymbol{T}_c(\boldsymbol{X}_0 : R,\theta,\phi,t)$ is a tensor composed of the static pressure and shear stress tensor of the continuous phase at point $(\boldsymbol{X}_0 : R,\theta,\phi)$ on the particle surface at time t, given by

$$\boldsymbol{T}_c(\boldsymbol{X}_0 : R,\theta,\phi,t) = P_c(\boldsymbol{X}_0 : R,\theta,\phi,t)\boldsymbol{I} + \boldsymbol{\tau}_c(\boldsymbol{X}_0 : R,\theta,\phi,t). \tag{3.5}$$

The time-averaged value of $\boldsymbol{f}_p$ for duration Λ can be given as

$$\overline{\boldsymbol{f}_p^{\Lambda}}(\boldsymbol{X}_0) = -\int_0^{\theta} \mathrm{d}\theta \int_0^{2\pi} \mathrm{d}\phi\, [\sin\theta\, R^2 \boldsymbol{n}(\theta,\phi)\cdot \overline{\boldsymbol{T}_c^{\Lambda}}(\boldsymbol{X}_0 : R,\theta,\phi)]. \tag{3.6}$$

Here, $\overline{\boldsymbol{T}_c^{\Lambda}}(\boldsymbol{X}_0 : R,\theta,\phi)$ means the time-averaged value of $\boldsymbol{T}_c$ on a particle surface at point $(\boldsymbol{X}_0 : R,\theta,\phi)$ precisely defined in Appendix B of the supplementary material, and $\overline{\boldsymbol{f}_p^{\Lambda}}(\boldsymbol{X}_0)$ is the time-averaged value of $\boldsymbol{f}_p(\boldsymbol{X}_0,t)$ for the duration when the particle centre is at point $\boldsymbol{X}_0$ during total time length Λ.

Now, the conventional interaction term can be expressed by the following surface integration:

$$\begin{aligned} &-\frac{1}{\Lambda}\int_0^{\pi}\int_0^{2\pi} \mathrm{d}\phi\, [\sin\theta\, \boldsymbol{n}(\theta,\phi)\cdot \overline{\boldsymbol{T}_c^{\Lambda}}(\boldsymbol{X}_0 : R,\theta,\phi)\lambda_R(\boldsymbol{X}_0)R^2] \\ &\quad = \frac{V_p\lambda_R(\boldsymbol{X}_0)}{\Lambda}\frac{1}{V_p}\overline{\boldsymbol{f}_p^{\Lambda}}(\boldsymbol{X}_0) \approx \frac{\Lambda_d(\boldsymbol{X}_0)}{\Lambda}\frac{1}{V_p}\overline{\boldsymbol{f}_p^{\Lambda}} = \epsilon(\boldsymbol{X}_0)\frac{1}{V_p}\overline{\boldsymbol{f}_p^{\Lambda}}. \end{aligned} \tag{3.7}$$

Here, V_p is the volume of a particle, and an approximation (F 5) derived in Appendix F of the supplementary material has been used. The final expression on the right-hand side of (3.7) coincides with the conventional interaction term. In the integrand of the surface integration, the surface force tensor $\overline{\boldsymbol{T}_c^{\Lambda}}$ is given at point $(\boldsymbol{X}_0 : R,\theta,\phi)$, which is on the surface of a sphere centred at $\boldsymbol{X}_0$, and λ_R is given at $\boldsymbol{X}_0$, which is the centre of the sphere.

3.3. *The 'inside-out' property of* $\lim_{V\to\boldsymbol{X}_0}(1/V)\overline{\boldsymbol{F}_{R,S}^{V}}^{\Lambda}$

In this section the intrinsic property of $\lim_{V\to\boldsymbol{X}_0}(1/V)\overline{\boldsymbol{F}_{R,S}^{V}}^{\Lambda}$ is illustrated schematically. Consider the particle surfaces in a control volume smaller than the particle size. Many particle surfaces come in and go out during total time length Λ, as shown in figure 3.

We observe that the particle centres for surfaces observed in the control volume gather, in the limit $V\to\boldsymbol{X}_0$, on the surface of a sphere with radius R with its centre at $\boldsymbol{X}_0$. Consequently, the value of $\lim_{V\to\boldsymbol{X}_0}(1/V)\overline{\boldsymbol{F}_{R,S}^{V}}^{\Lambda}$ is given by a surface integration over the surface of a sphere with radius R and with centre at $\boldsymbol{X}_0$, where $\overline{\boldsymbol{T}_c^{\Lambda}}$ in the integrand is specified at the centre of the sphere, that is, $(\boldsymbol{X}_0 - R\boldsymbol{n}(\theta,\phi) : R,\theta,\phi)$, and λ_R on the surface of the sphere, that is, $\boldsymbol{X}_0 - R\boldsymbol{n}(\theta,\phi)$:

$$\begin{aligned} \lim_{V\to\boldsymbol{X}_0}\frac{1}{V}\overline{\boldsymbol{F}_{R,S}^{V}}^{\Lambda} = -\frac{1}{\Lambda}\int_0^{\pi}\mathrm{d}\theta\int_0^{2\pi}\mathrm{d}\phi\, [R^2\sin\theta\,\lambda_R(\boldsymbol{X}_0 - R\boldsymbol{n}(\theta,\phi)) \\ \times \boldsymbol{n}(\theta,\phi)\cdot\overline{\boldsymbol{T}_c^{\Lambda}}(\boldsymbol{X}_0 - R\boldsymbol{n}(\theta,\phi) : R,\theta,\phi)]. \end{aligned} \tag{3.8}$$

A rigorous derivation of (3.8) is given in Appendix B of the supplementary material. It is shown in Appendix C therein that the expression on the right-hand side of (3.8) is identical to the impulse term in the Navier–Stokes equations suitably time-averaged for multiphase flow (Ishii 1975; Ueyama & Miyauchi 1976).

https://doi.org/10.1017/jfm.2011.452 Published online by Cambridge University Press

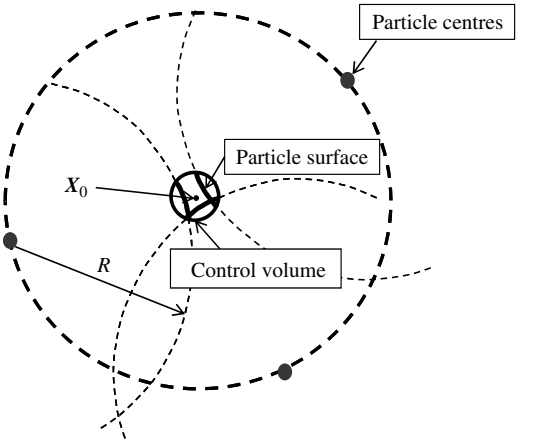


FIGURE 3. Particle surfaces in a small control volume.

In (3.8), the value of $\overline{\boldsymbol{T}_c^{\Lambda}}$ is given at point $(\boldsymbol{X}_0 - R\boldsymbol{n}(\theta,\phi) : R, \theta, \phi)$, which is a point (R, θ, ϕ) in the spherical coordinate system with its origin at $\boldsymbol{X}_0 - R\boldsymbol{n}(\theta,\phi)$, that is, the centre of the sphere, $\boldsymbol{X}_0$, and the value of λ_R is given at $\boldsymbol{X}_0 - R\boldsymbol{n}(\theta,\phi)$, which is on the surface of the sphere. The positions assigned for $\overline{\boldsymbol{T}_c^{\Lambda}}$ and λ_R are exchanged with each other from those in (3.7) for the conventional interaction term. This is the intrinsic property of the interaction term $\lim_{V\to\boldsymbol{X}_0}(1/V)\overline{\boldsymbol{F}_{R,S}^{V}}^{\Lambda}$, which rigorously fits to the two-fluid model equations. This will be called the 'inside-out' property below, and the term $\lim_{V\to\boldsymbol{X}_0}(1/V)\overline{\boldsymbol{F}_{R,S}^{V}}^{\Lambda}$ will occasionally be referred to as the 'inside-out' interaction term. This property of the interaction term has not been recognized before.

The mathematical expression of $\lim_{V\to\boldsymbol{X}_0}(1/V)\overline{\boldsymbol{F}_{R,S}^{V}}^{\Lambda}$ for non-spherical particles is

$$\lim_{V\to\boldsymbol{X}_0}\frac{1}{V}\overline{\boldsymbol{F}_{R,S}^{V}}^{\Lambda} = -\frac{1}{\Lambda}\int_0^{\pi}\mathrm{d}\theta\int_0^{2\pi}\mathrm{d}\phi\,[\{R(\theta,\phi)\}^2\,C(\theta,\phi)\sin\theta\,\lambda_R(\boldsymbol{X}_0 - R(\theta,\phi)\boldsymbol{i}_r(\theta,\phi))$$
$$\times\,\boldsymbol{n}(\theta,\phi)\cdot\overline{\boldsymbol{T}_c^{\Lambda}}(\boldsymbol{X}_0 - R(\theta,\phi)\boldsymbol{i}_r(\theta,\phi) : R(\theta,\phi),\theta,\phi)], \tag{3.9}$$

in a similar way as for spherical particles; this expression is derived in Appendix D of the supplementary material. Here, a point on a particle surface with its reference point at $\boldsymbol{X}_0$ is given as $(\boldsymbol{X}_0 : R(\theta,\phi), \theta, \phi)$, and $C(\theta,\phi)$ is a correction factor corresponding to the shape of the particle surface suitably defined so that the surface area element at $(R(\theta,\phi), \theta, \phi)$ is precisely given as $C(\theta,\phi)\,\{R(\theta,\phi)\}^2\sin\theta\,\mathrm{d}\theta\,\mathrm{d}\phi$. The symbol $\boldsymbol{n}(\theta,\phi)$ is a unit normal vector directed outwards on a particle surface at point $(\boldsymbol{X}_0 : R(\theta,\phi), \theta, \phi)$, and $\boldsymbol{i}_r(\theta,\phi)$ is a unit vector along the r axis at the angular coordinate (θ,ϕ).

3.4. *Interaction term in terms of force acting on a drop*

The drag force, lift force and virtual mass force are forces acting on a particle due to motion of the particle relative to the surrounding fluid. In general, the values of the static pressure and shear stress tensor on a particle surface are different from the values in the bulk fluid. Routine analysis is available in the literature of the drag force, lift force and virtual mass force so as to determine the difference between the surface value and the bulk value of the static pressure and shear stress tensor. The time-averaged values of $\boldsymbol{T}_c$ at spherical coordinates (R, θ, ϕ) on the surface, $\overline{\boldsymbol{T}_c^{\Lambda}}$, and

https://doi.org/10.1017/jfm.2011.452 Published online by Cambridge University Press

the bulk value, $\overline{\boldsymbol{T}_c}^c$, are given as functions of position in this work, and it is convenient to define their difference at a given point as follows:

$$\Delta\overline{\boldsymbol{T}_c}^{\Lambda}(\boldsymbol{X}-R\boldsymbol{n}(\theta,\phi):R,\theta,\phi)=\overline{\boldsymbol{T}_c}^{\Lambda}(\boldsymbol{X}-R\boldsymbol{n}(\theta,\phi):R,\theta,\phi)-\overline{\boldsymbol{T}_c}^c(\boldsymbol{X}). \tag{3.10}$$

In (3.10), the point $(\boldsymbol{X}-R\boldsymbol{n}(\theta,\phi):R,\theta,\phi)$ in spherical coordinates with its origin at $\boldsymbol{X}-R\boldsymbol{n}(\theta,\phi)$ is the same as the point $\boldsymbol{X}$ in Cartesian coordinates.

The contribution of $\Delta\overline{\boldsymbol{T}_c}^{\Lambda}$ on an entire drop surface with centre at $\boldsymbol{X}_0$, which is denoted as $\overline{\boldsymbol{f}_p}^{\Delta\boldsymbol{T}}(\boldsymbol{X}_0)$, is given by

$$\overline{\boldsymbol{f}_p}^{\Delta\boldsymbol{T}}(\boldsymbol{X}_0)=-\int_0^{\pi}\mathrm{d}\theta\int_0^{2\pi}\mathrm{d}\phi\,[\sin\theta\,\boldsymbol{n}(\theta,\phi)\cdot\Delta\overline{\boldsymbol{T}_c}^{\Lambda}(\boldsymbol{X}_0:R,\theta,\phi)R^2]. \tag{3.11}$$

Standard analyses of the drag force, lift force and virtual mass force can be applied to $\overline{\boldsymbol{f}_p}^{\Delta\boldsymbol{T}}$.

Let us express (3.8) in terms of $\Delta\overline{T_c}^{\Lambda}$. From (3.8) and (3.10), we have

$$\begin{aligned}\lim_{V\to X_0}\frac{1}{V}\overline{\boldsymbol{F}_{R,S}^{V}}^{\Lambda}=&-\frac{1}{\Lambda}\int_0^{\pi}\mathrm{d}\theta\int_0^{2\pi}\mathrm{d}\phi\,[\sin\theta\,\boldsymbol{n}(\theta,\phi)\cdot\Delta\overline{\boldsymbol{T}_c}^{\Lambda}(\boldsymbol{X}_0-R\boldsymbol{n}(\theta,\phi):R,\theta,\phi)\\&\times\lambda_R(\boldsymbol{X}_0-R\boldsymbol{n}(\theta,\phi))R^2]\\&-\frac{1}{\Lambda}\int_0^{\pi}\mathrm{d}\theta\int_0^{2\pi}\mathrm{d}\phi\,[\sin\theta\,\boldsymbol{n}(\theta,\phi)\cdot\overline{\boldsymbol{T}_c}^c(\boldsymbol{X}_0)\\&\times\lambda_R(\boldsymbol{X}_0-R\boldsymbol{n}(\theta,\phi))R^2].\end{aligned} \tag{3.12}$$

The first term on the right-hand side does not directly correspond to $\overline{\boldsymbol{f}_p}^{\Delta\boldsymbol{T}}$ because of its 'inside-out' property. The 'inside-out' property of the first term can be treated by using Taylor expansion to shift the points at which $\Delta\overline{\boldsymbol{T}_c}^{\Lambda}$ and λ_R are specified. Upon neglecting higher-order terms, we have

$$\begin{aligned}&\Delta\overline{\boldsymbol{T}_c}^{\Lambda}(\boldsymbol{X}_0-R\boldsymbol{n}(\theta,\phi):R,\theta,\phi)\\&\quad\approx\Delta\overline{\boldsymbol{T}_c}^{\Lambda}(\boldsymbol{X}_0:R,\theta,\phi)-R\frac{\Delta\overline{\boldsymbol{T}_c}^{\Lambda}(\boldsymbol{X}_0+\Delta r\,\boldsymbol{n}(\theta,\phi):R,\theta,\phi)-\Delta\overline{\boldsymbol{T}_c}^{\Lambda}(\boldsymbol{X}_0:R,\theta,\phi)}{\Delta r},\end{aligned} \tag{3.13}$$

$$\lambda_R(\boldsymbol{X}_0-R\boldsymbol{n}(\theta,\phi))\approx\lambda_R(\boldsymbol{X}_0)-R\boldsymbol{n}(\theta,\phi)\cdot(\nabla\lambda_R)|_{\boldsymbol{X}_0}. \tag{3.14}$$

The validity of the truncations made in (3.13) and (3.14) depends on the spatial variation of $\Delta\overline{\boldsymbol{T}_c}^{\Lambda}$ and λ_R on the scale of the diameter of the particle. When quadratic and higher-order terms cannot be neglected, it is necessary to modify (3.13) and (3.14); this is not investigated further here.

The second term on the right-hand side of (3.12) can be calculated, because the tensor $\overline{\boldsymbol{T}_c}^c(\boldsymbol{X}_0)$ is constant; it is

$$\begin{aligned}&-\frac{1}{\Lambda}\int_0^{\pi}\mathrm{d}\theta\int_0^{2\pi}\mathrm{d}\phi\,[\sin\theta\,\boldsymbol{n}(\theta,\phi)\cdot\overline{\boldsymbol{T}_c}^c(\boldsymbol{X}_0)\lambda_R(\boldsymbol{X}_0-R\boldsymbol{n}(\theta,\phi))R^2]\\&=\frac{1}{\Lambda}\int_0^{\pi}\mathrm{d}\theta\int_0^{2\pi}\mathrm{d}\phi\,[\sin\theta\,\boldsymbol{n}(\theta,\phi)\lambda_R(\boldsymbol{X}_0+R\boldsymbol{n}(\theta,\phi))R^2]\cdot\overline{\boldsymbol{T}_c}^c(\boldsymbol{X}_0)\\&\approx(\nabla\epsilon)|_{\boldsymbol{X}_0}\cdot\overline{\boldsymbol{T}_c}^c(\boldsymbol{X}_0)=(\nabla\epsilon)|_{\boldsymbol{X}_0}\overline{P_c}^c(\boldsymbol{X}_0)+(\nabla\epsilon)|_{\boldsymbol{X}_0}\cdot\overline{\boldsymbol{\tau}_c}^c(\boldsymbol{X}_0).\end{aligned} \tag{3.15}$$

A derivation of (3.15) is given in Appendix E of the supplementary material.

https://doi.org/10.1017/jfm.2011.452 Published online by Cambridge University Press

By using (3.10), the expression $\Delta\overline{\boldsymbol{T}_c^{\Lambda}}(\boldsymbol{X}_0 + \Delta r\,\boldsymbol{n}(\theta,\phi) : R,\theta,\phi) - \Delta\overline{\boldsymbol{T}_c^{\Lambda}}(\boldsymbol{X}_0 : R,\theta,\phi)$ in the second term on the right-hand side of (3.13) can be transformed to

$$\begin{aligned}
&\Delta\overline{\boldsymbol{T}_c^{\Lambda}}(\boldsymbol{X}_0 + \Delta r\,\boldsymbol{n}(\theta,\phi) : R,\theta,\phi) - \Delta\overline{\boldsymbol{T}_c^{\Lambda}}(\boldsymbol{X}_0 : R,\theta,\phi)\\
&\quad = \{\overline{\boldsymbol{T}_c^{\Lambda}}(\boldsymbol{X}_0 + \Delta r\,\boldsymbol{n}(\theta,\phi) : R,\theta,\phi) - \overline{\boldsymbol{T}_c^{\Lambda}}(\boldsymbol{X}_0 : R,\theta,\phi)\}\\
&\quad - \{\overline{\boldsymbol{T}_c}^{c}(\boldsymbol{X}_0 + (R+\Delta r)\boldsymbol{n}(\theta,\phi)) - \overline{\boldsymbol{T}_c}^{c}(\boldsymbol{X}_0 + R\boldsymbol{n}(\theta,\phi))\}. \qquad (3.16)
\end{aligned}$$

In general, the time-averaged value of the tensor $\boldsymbol{T}_c$ at fixed spherical coordinates (R,θ,ϕ) on the surface of a particle with centre at $\boldsymbol{X}_0$, that is, $\overline{\boldsymbol{T}_c^{\Lambda}}(\boldsymbol{X}_0 : R,\theta,\phi)$, is different from the time-averaged value of $\boldsymbol{T}_c$ in the continuous phase at the same point, that is, $\overline{\boldsymbol{T}_c}^{c}(\boldsymbol{X}_0 + R\boldsymbol{n}(\theta,\phi))$. As $\overline{\boldsymbol{T}_c}^{c}(\boldsymbol{X}_0 + R\boldsymbol{n}(\theta,\phi))$ increases, so does $\overline{\boldsymbol{T}_c^{\Lambda}}(\boldsymbol{X}_0 : R,\theta,\phi)$. The difference between the values of $\overline{\boldsymbol{T}_c}^{c}(\boldsymbol{X}_0 + R\boldsymbol{n}(\theta,\phi))$ and $\overline{\boldsymbol{T}_c^{\Lambda}}(\boldsymbol{X}_0 : R,\theta,\phi)$ depends on the time-averaged relative flow field between the drop with centre at $\boldsymbol{X}_0$ and the surrounding continuous phase. Since the time-averaged relative flow field should be common to neighbouring drops within a range of drop sizes, we expect that the difference between $\overline{\boldsymbol{T}_c^{\Lambda}}(\boldsymbol{X}_0 + \Delta r\,\boldsymbol{n}(\theta,\phi) : R,\theta,\phi)$ and $\overline{\boldsymbol{T}_c}^{c}(\boldsymbol{X}_0 + (R+\Delta r)\boldsymbol{n}(\theta,\phi))$ is almost the same as the difference between $\overline{\boldsymbol{T}_c^{\Lambda}}(\boldsymbol{X}_0 : R,\theta,\phi)$ and $\overline{\boldsymbol{T}_c}^{c}(\boldsymbol{X}_0 + R\boldsymbol{n}(\theta,\phi))$. It now follows from (3.15) that

$$\begin{aligned}
&\Delta\overline{\boldsymbol{T}_c^{\Lambda}}(\boldsymbol{X}_0 + \Delta r\,\boldsymbol{n}(\theta,\phi) : R,\theta,\phi) - \Delta\overline{\boldsymbol{T}_c^{\Lambda}}(\boldsymbol{X}_0 : R,\theta,\phi)\\
&\quad = \{\overline{\boldsymbol{T}_c^{\Lambda}}(\boldsymbol{X}_0 + \Delta r\,\boldsymbol{n}(\theta,\phi) : R,\theta,\phi) - \overline{\boldsymbol{T}_c}^{c}(\boldsymbol{X}_0 + (R+\Delta r)\boldsymbol{n}(\theta,\phi))\}\\
&\qquad - \{\overline{\boldsymbol{T}_c^{\Lambda}}(\boldsymbol{X}_0 : R,\theta,\phi) - \overline{\boldsymbol{T}_c}^{c}(\boldsymbol{X}_0 + R\boldsymbol{n}(\theta,\phi))\}\\
&\quad \approx 0. \qquad (3.17)
\end{aligned}$$

From (3.13) and (3.17), we have

$$\Delta\overline{\boldsymbol{T}_c^{\Lambda}}(\boldsymbol{X}_0 - R\boldsymbol{n}(\theta,\phi) : R,\theta,\phi) \approx \Delta\overline{\boldsymbol{T}_c^{\Lambda}}(\boldsymbol{X}_0 : R,\theta,\phi). \qquad (3.18)$$

From (3.14), (3.15) and (3.18), equation (3.12) becomes

$$\begin{aligned}
\lim_{V\to X_0}\frac{1}{V}\overline{\boldsymbol{F}_{R,S}^{V}}^{\Lambda} \approx &-\frac{1}{\Lambda}\int_0^{\pi}\mathrm{d}\theta\int_0^{2\pi}\mathrm{d}\phi\,[\sin\theta\,\boldsymbol{n}(\theta,\phi)\cdot\Delta\overline{\boldsymbol{T}_c^{\Lambda}}(\boldsymbol{X}_0 : R,\theta,\phi)\lambda_R(\boldsymbol{X}_0)R^2]\\
&+\frac{1}{\Lambda}\int_0^{\pi}\mathrm{d}\theta\int_0^{2\pi}\mathrm{d}\phi\,[\sin\theta\,\boldsymbol{n}(\theta,\phi)\cdot\Delta\overline{\boldsymbol{T}_c}^{c}(\boldsymbol{X}_0)\{\boldsymbol{n}(\theta,\phi)\cdot(\nabla\lambda_R)|_{\boldsymbol{X}_0}\}R^3]\\
&+(\nabla\epsilon)|_{\boldsymbol{X}_0}\overline{\boldsymbol{P}_c}^{c}(\boldsymbol{X}_0) + (\nabla\epsilon)|_{\boldsymbol{X}_0}\cdot\overline{\tau_c}^{c}(\boldsymbol{X}_0). \qquad (3.19)
\end{aligned}$$

The first term on the right-hand side of (3.19) can be calculated; details are set out in Appendix F of the supplementary material, and the result is

$$\lim_{V\to X_0}\frac{1}{V}\overline{\boldsymbol{F}_{R,S}^{V}}^{\Lambda} \approx \epsilon(\boldsymbol{X}_0)\frac{\overline{\boldsymbol{f}_p^{\Delta T}}(\boldsymbol{X}_0)}{V_p} + \boldsymbol{F}_v + (\nabla\epsilon)|_{\boldsymbol{X}_0}\overline{\boldsymbol{P}_c}^{c}(\boldsymbol{X}_0) + (\nabla\epsilon)|_{\boldsymbol{X}_0}\overline{\tau_c}^{c}(\boldsymbol{X}_0). \qquad (3.20)$$

Equation (3.20) gives the interaction term $\lim_{V\to X_0}(1/V)\overline{\boldsymbol{F}_{R,S}^{V}}^{\Lambda}$ for the two-fluid model equations, based on time averaging. Here, $\boldsymbol{F}_v$ is the second term on the right-hand side of (3.19), the value of which can be calculated by using the spatial distribution of the local holdup and distributions of pressure and shear stress on a particle surface:

$$\begin{aligned}
\boldsymbol{F}_v = &\frac{1}{\Lambda}\int_0^{\pi}\mathrm{d}\theta\int_0^{2\pi}\mathrm{d}\phi\,[R^3\sin\theta\,\{\boldsymbol{n}(\theta,\phi)\cdot(\nabla\lambda_R)|_{\boldsymbol{X}_0}\}\\
&\times\boldsymbol{n}(\theta,\phi)\cdot\Delta\overline{\boldsymbol{T}_c^{\Lambda}}(\boldsymbol{X}_0 : R,\theta,\phi)]. \qquad (3.21)
\end{aligned}$$

https://doi.org/10.1017/jfm.2011.452 Published online by Cambridge University Press

The first term on the right-hand side of (3.20) is the same as the conventional interaction term. Standard analyses of the drag force, lift force and virtual mass force for a single particle in a flow field can now be applied to $\overline{\boldsymbol{f}_p^{\Delta T}}(\boldsymbol{X}_0)$.

The second term $\boldsymbol{F}_v$ is introduced to compensate for the discrepancy between $\lim_{V\to X_0}(1/V)\overline{\boldsymbol{F}_{R,S}^{V}}^{\Lambda}$, which is the interaction term in the two-fluid model equations based on time averaging, and the conventional interaction term $\epsilon(\boldsymbol{X}_0)\overline{\boldsymbol{f}_p^{\Delta T}}(\boldsymbol{X}_0)/V_d$. This term will be referred to henceforth as a virtual force term, because it does not represent any real physical phenomena. It is nevertheless possible to interpret the term. As stated in Appendix F, the main property of $\boldsymbol{F}_v$ can be given by

$$\boldsymbol{F}_v \approx -R\left(\frac{\partial \epsilon}{\partial Z}\right)\bigg|_{X_0} \frac{c^+\overline{\boldsymbol{f}_p^{\Delta T+}}(\boldsymbol{X}_0) - c^-\overline{\boldsymbol{f}_p^{\Delta T-}}(\boldsymbol{X}_0)}{V_p}. \tag{3.22}$$

Here, the Z axis is chosen in the direction of $\nabla\epsilon$. The terms $\overline{\boldsymbol{f}_p^{\Delta T+}}(\boldsymbol{X}_0)$ and $\overline{\boldsymbol{f}_p^{\Delta T-}}(\boldsymbol{X}_0)$ are forces acting on the two hemispherical surfaces of the particle that have positive and negative values of Z, respectively. The parameters c^+ and c^- are fitting parameters; they are positive and less than unity, and represent the effect of the weight function $\cos\theta$ in the surface integration over the hemisphere surface for positive and negative values of Z, respectively. Since $\cos\theta$ is an odd function about the value $\theta = \pi/2$, we expect that $c^+ \approx c^- \approx c$, and the term then simplifies to $-cR(\partial\epsilon/\partial Z)|_{X_0}(\overline{\boldsymbol{f}_p^{\Delta T+}}(\boldsymbol{X}_0) - \overline{\boldsymbol{f}_p^{\Delta T-}}(\boldsymbol{X}_0))/V_p$, with a readier physical interpretation. The forces acting on the hemispherical surfaces consequently emerge as expected from the discussion based on figure 1. The virtual force term $\boldsymbol{F}_v$ becomes significant for flow with spatial gradients of the local holdup and averaged velocity, as will be estimated below in the case of creeping flow around spherical solid particles and gas–liquid dispersed flow with spherical cap bubbles. It is urgent to know the distribution of $\Delta\overline{\boldsymbol{T}_c}^{\Lambda}$ on a particle surface, on which we can calculate the value of the virtual force term.

The third term on the right-hand side of (3.20) is similar to the result of Kolev (2007) in rearranging surface integrals for two-fluid model equations based on volume averaging, which is crucial to excluding local holdup from the differential operator ∇ in the static pressure term in the two-fluid model equation.

The fourth term on the right-hand side of (3.20) arises from the definition of the force acting on a particle $\overline{\boldsymbol{f}_p^{\Delta T}}(\boldsymbol{X}_0)$ given by (3.11), since $\Delta\overline{\boldsymbol{T}_c}^{\Lambda}$, which is the difference between time-averaged values of tensor $\boldsymbol{T}_c = P_c\boldsymbol{I} + \boldsymbol{\tau}_c$ on a particle surface and in the bulk of the continuous phase, was taken to define the force acting on a particle. This term will make a small modification in the shear stress term in the two-fluid model equation, as shown later.

4. Equation of motion for a particle in dispersed two-phase flow

Consider the equation of motion for a particle in a dispersed two-phase flow, so as to clarify the physical interpretations of the terms in the equation prior to consideration of the virtual force term. The density of a particle is treated as constant in this section for the sake of simplicity. The velocity of a particle is to be determined from the equation of motion with appropriate initial condition,

$$\frac{\mathrm{d}}{\mathrm{d}t}\int_{V_p}\rho_p\boldsymbol{u}_p\,\mathrm{d}V = -\oint_{S_p}\boldsymbol{n}P_c\,\mathrm{d}S - \oint_{S_p}\boldsymbol{n}\cdot\boldsymbol{\tau}_c\,\mathrm{d}S + \boldsymbol{g}\int_{V_p}\rho_p\,\mathrm{d}V. \tag{4.1}$$

https://doi.org/10.1017/jfm.2011.452 Published online by Cambridge University Press

Here, V_p and S_p denote the volume and surface of a particle, ρ_p and $\boldsymbol{u}_p$ are the density and velocity of the particle, and $\boldsymbol{n}$ is a unit normal vector directed outwards on the surface S_p. The right-hand side of (4.1) is a sum of forces acting on the particle, which usually are the drag force, the lift force, the buoyancy, the virtual mass force, the Basset force, and so on, but they are not explicit. The buoyancy term can be picked out of the equation of motion by using the Navier–Stokes equation for the flow field without the particle. For a flow field $\boldsymbol{u}_c$, we have

$$\frac{\mathrm{d}}{\mathrm{d}t}\int_{V_p}\rho_c\boldsymbol{u}_c\,\mathrm{d}V=-\oint_{S_p}\boldsymbol{n}P_c^b\,\mathrm{d}S-\oint_{S_p}\boldsymbol{n}\cdot\boldsymbol{\tau}_c^b\,\mathrm{d}S+\boldsymbol{g}\int_{V_p}\rho_c\,\mathrm{d}V. \tag{4.2}$$

Here, S_p is a conceptual surface moving with velocity $\boldsymbol{u}_c$ in the flow field without the particle, so that P_c^b and $\boldsymbol{\tau}_c^b$ are the static pressure and shear stress tensor in the bulk fluid, not at the particle surface. The left-hand side of (4.2) becomes zero when the flow field is stationary. From (4.1) and (4.2), the stationary flow field conforms to the relation

$$\frac{\mathrm{d}}{\mathrm{d}t}\int_{V_p}\rho_p\boldsymbol{u}_p\,\mathrm{d}V=-\oint_{S_p}\boldsymbol{n}\Delta P_c\,\mathrm{d}S-\oint_{S_p}\boldsymbol{n}\cdot\Delta\boldsymbol{\tau}_c\,\mathrm{d}S+\boldsymbol{g}\int_{V_p}(\rho_p-\rho_c)\,\mathrm{d}V. \tag{4.3}$$

Here, $\Delta P_c=P_c-P_c^b$ and $\Delta\boldsymbol{\tau}_c=\boldsymbol{\tau}_c-\boldsymbol{\tau}_c^b$ are the excess pressure and the excess shear stress tensor caused by the particle. The third term on the right-hand side is the buoyancy term, which means a weight reduction corresponding to the fluid weight displaced by the particle. Then, the drag force, the lift force, the virtual mass force and the Basset force correspond to the first and second terms on the right-hand side of (4.3), which are contributions of the excess pressure and the excess shear stress on the particle surface.

We expect the time-averaged expression of (4.1) for particles appearing at the point of interest during the total duration Λ to be

$$\frac{\mathrm{d}}{\mathrm{d}t}\int_{V_p}\rho_p\overline{\boldsymbol{u}_p^{\Lambda}}\,\mathrm{d}V=-\oint_{S_p}\boldsymbol{n}\cdot\overline{\boldsymbol{T}_c^{\Lambda}}\,\mathrm{d}S+\boldsymbol{g}\int_{V_p}\rho_p\,\mathrm{d}V. \tag{4.4}$$

Here, $\overline{\boldsymbol{T}_c^{\Lambda}}$ is the time-averaged value of $\boldsymbol{T}_c$ on the surface of the particle (specified in detail in Appendix B of the supplementary material), and $\overline{\boldsymbol{u}_p^{\Lambda}}$ is the time-averaged moving velocity of a particle centre (see Appendix G therein). There is an exact relation between $\overline{\boldsymbol{u}_p^{\Lambda}}$ and $\overline{\boldsymbol{u}_d}^{d}$ (see Appendix G):

$$\begin{aligned}\epsilon(\boldsymbol{X}_0)\Lambda\,\overline{\boldsymbol{u}_d}^{d}(\boldsymbol{X}_0)&=\int_0^{\pi}\mathrm{d}\theta\int_0^{2\pi}\mathrm{d}\phi\left[\int_0^{R}r^2\sin\theta\,\lambda_R(\boldsymbol{X}_0:r,\theta,\phi)\overline{\boldsymbol{u}_p^{\Lambda}}(\boldsymbol{X}_0:r,\theta,\phi)\,\mathrm{d}r\right]\\&=\int_{V_p}\lambda_R(\boldsymbol{X})\overline{\boldsymbol{u}_p^{\Lambda}}(\boldsymbol{X})\,\mathrm{d}V.\end{aligned} \tag{4.5}$$

By using a Taylor expansion to shift the position where λ_R and $\overline{\boldsymbol{u}_p^{\lambda}}$ are specified and neglecting higher-order terms, (4.5) approximates to (see Appendix G)

$$\overline{\boldsymbol{u}_d}^{d}\approx\overline{\boldsymbol{u}_p^{\Lambda}}+\frac{R^2}{5}\frac{(\nabla\epsilon)}{\epsilon}\cdot(\nabla\overline{\boldsymbol{u}_p^{\Lambda}}). \tag{4.6}$$

When neither the local holdup ϵ nor the time-averaged moving velocity of a particle $\overline{\boldsymbol{u}_p^{\Lambda}}$ are homogeneous in space, the values of $\overline{\boldsymbol{u}_p^{\Lambda}}$ and $\overline{\boldsymbol{u}_d}^{d}$ may not be the same. The difference in physical meaning and value of $\overline{\boldsymbol{u}_p^{\Lambda}}$ and $\overline{\boldsymbol{u}_d}^{d}$ has not been considered

https://doi.org/10.1017/jfm.2011.452 Published online by Cambridge University Press

in previous work, except by Kulkarni (2008). Kulkarni mentioned that a parabolic radial distribution of gas holdup in bubble columns in a recirculating turbulent flow regime is realized due to a balance between the radial movement of the bubbles and the counter-diffusion flux of the bubbles. A clear understanding of the physical quantities $\overline{\boldsymbol{u}_p^{\Lambda}}$ and $\overline{\boldsymbol{u}_d}^d$ is central in constructing Euler–Euler and Euler–Lagrange types of simulators in considering diffusion phenomena of particles. This is not considered further in the present paper.

For a particle in the dispersed two-phase flow, expressions in the literature for the drag force, lift force, buoyancy, virtual mass term and Basset force are expected to be applied, and have actually been used (Zhang, Deen & Kuipers 2006; Hibiki & Ishii 2007; Tabib *et al.* 2008). It is now necessary to relate the terms in (4.4) to the drag force, lift force, buoyancy, virtual mass term and Basset force term.

The buoyancy term can also be picked out of the equation of motion by using the Navier–Stokes equation for the surrounding fluid phase. For a particle in the dispersed two-phase flow, the Navier–Stokes equation for the time-averaged velocity vector $\overline{\boldsymbol{u}_c}^c$ of the surrounding flow is obtained by summing the time-averaged Navier–Stokes equations for the continuous and dispersed phases:

$$\rho_m \frac{\partial}{\partial t}\overline{\boldsymbol{u}_c}^c + \rho_m \overline{\boldsymbol{u}_c}^c \cdot (\nabla \overline{\boldsymbol{u}_c}^c) \approx -\nabla(\overline{P_c}^c \boldsymbol{I} + \overline{\boldsymbol{\tau}_c}^c) - \nabla \cdot \overline{\boldsymbol{\tau}_R} + \rho_m \boldsymbol{g} - \epsilon\rho_d \overline{\boldsymbol{u}_R} \cdot (\nabla \overline{\boldsymbol{u}_c}^c). \quad (4.7)$$

Here, $\rho_m = \epsilon\rho_d + (1-\epsilon)\rho_c$ is the mean density of the two-phase flow, $\overline{\boldsymbol{\tau}_R} = (1-\epsilon)\rho_c \overline{\boldsymbol{u}_c' \boldsymbol{u}_c'}^c + \epsilon\rho_d \overline{\boldsymbol{u}_d' \boldsymbol{u}_d'}^d$ is the Reynolds stress of the two-phase flow, and $\overline{\boldsymbol{u}_R} = \overline{\boldsymbol{u}_d}^d - \overline{\boldsymbol{u}_c}^c$ is a relative velocity vector between the time-averaged velocity vectors of the dispersed and continuous phases. Equation (4.7) is derived in Appendix H of the supplementary material.

For a closed surface S_p moving with velocity $\overline{\boldsymbol{u}_c}^c$ in a space of (4.7), we have

$$\int_{V_p} \left(\rho_m \frac{\mathrm{d}}{\mathrm{d}t}\overline{\boldsymbol{u}_c}^c\right) \mathrm{d}V \approx -\oint_{S_p} \boldsymbol{n} \cdot \overline{\boldsymbol{T}_c}^c \,\mathrm{d}S - \oint_{S_p} \boldsymbol{n} \cdot \overline{\boldsymbol{\tau}_R} \,\mathrm{d}S + \int_{V_p} \rho_m \boldsymbol{g} \,\mathrm{d}V. \quad (4.8)$$

Here, $\overline{\boldsymbol{u}_c}^c$ has been taken to be constant in the direction of $\overline{\boldsymbol{u}_R}$, for simplicity. This assumption is valid for the recirculating turbulent flow regime in bubble columns (Ueyama & Miyauchi 1979), where both $\overline{\boldsymbol{u}_d}^d$ and $\overline{\boldsymbol{u}_c}^c$ are axially directed, and $\overline{\boldsymbol{u}_c}^c$ is constant to the axial direction. Since the closed surface S_p in (4.8) is moving with velocity $\overline{\boldsymbol{u}_c}^c$, the mean density in S_p is constant. Equation (4.8) can then be transformed to

$$\frac{\mathrm{d}}{\mathrm{d}t}\int_{V_p} \rho_m \overline{\boldsymbol{u}_c}^c \,\mathrm{d}V \approx -\oint_{S_p} \boldsymbol{n} \cdot \overline{\boldsymbol{T}_c}^c \,\mathrm{d}S - \oint_{S_p} \boldsymbol{n} \cdot \overline{\boldsymbol{\tau}_R} \,\mathrm{d}S + \int_{V_p} \rho_m \boldsymbol{g} \,\mathrm{d}V. \quad (4.9)$$

From (4.4) and (4.9), we have

$$\begin{aligned}\frac{\mathrm{d}}{\mathrm{d}t}\int_{V_p} \rho_p \overline{\boldsymbol{u}_p^{\Lambda}} \,\mathrm{d}V \approx &-\frac{\mathrm{d}}{\mathrm{d}t}\int_{V_p} \rho_m \overline{\boldsymbol{u}_c}^c \,\mathrm{d}V - \oint_{S_p} \boldsymbol{n} \cdot \overline{\boldsymbol{\tau}_R} \,\mathrm{d}S \\ &- \oint_{S_p} \boldsymbol{n} \cdot \Delta\overline{\boldsymbol{T}_c^{\Lambda}} \,\mathrm{d}S + \boldsymbol{g}\int_{V_p} (\rho_p - \rho_m) \,\mathrm{d}V. \end{aligned} \quad (4.10)$$

Here, $\Delta\overline{\boldsymbol{T}_c^{\Lambda}}$ is the difference between the time-averaged values of $\boldsymbol{T}_c$ on a particle surface and in the bulk surrounding fluid, as defined by (3.10). The first and second terms on the right-hand side are not forces acting on a particle in the two-phase mixture, but are forces acting on a conceptual surface in the space of (4.7) moving

https://doi.org/10.1017/jfm.2011.452 Published online by Cambridge University Press

with fluid velocity $\overline{\boldsymbol{u}_c}^c$. These terms have been introduced to obtain the fourth term, which is the buoyancy term. The derivation of (4.10) requires that the reference density in the buoyancy term should be the mean density of the multiphase mixture for a particle in dispersed two-phase flow.

Since the virtual mass force and the Basset force represent contributions due to acceleration, the third term on the right-hand side of (4.10) is made up of the drag force, lift force, virtual mass force and Basset force, when the value of the left-hand side is not zero.

When the two-phase flow is stationary, the first term on the right-hand side of (4.10) vanishes:

$$\frac{\mathrm{d}}{\mathrm{d}t}\int_{V_p}\rho_p\overline{\boldsymbol{u}_p}^{\Lambda}\,\mathrm{d}V \approx -\oint_{S_p}\boldsymbol{n}\cdot\overline{\boldsymbol{\tau}_R}\,\mathrm{d}S - \oint_{S_p}\boldsymbol{n}\cdot\Delta\overline{\boldsymbol{T}_c}^{\Lambda}\,\mathrm{d}S + \boldsymbol{g}\int_{V_p}(\rho_p-\rho_m)\,\mathrm{d}V. \quad (4.11)$$

The first term on the right-hand side of (4.11) remains, though it is not a force acting on a particle surface. This situation is the same as discussed by Zhang & Prosperetti (1994) in deriving the ensemble average of the equation of motion for a particle. They introduced a stress term originating from Reynolds stress, together with the procedure excluding the local void fraction from the ensemble mean of the pressure gradient.

When the particle is moving at its terminal velocity, we have

$$0 \approx -\oint_{S_p}\boldsymbol{n}\cdot\overline{\boldsymbol{\tau}_R}\,\mathrm{d}S - \oint_{S_p}\boldsymbol{n}\cdot\Delta\overline{\boldsymbol{T}_c}^{\Lambda}\,\mathrm{d}S + \boldsymbol{g}\int_{V_p}(\rho_p-\rho_m)\,\mathrm{d}V. \quad (4.12)$$

The virtual mass force and the Basset force are zero in this case, but the Reynolds stress term remains. If we take the buoyancy term as the third term on the right-hand side, the first term should be taken into the equation of motion, together with the second term, corresponding to the drag and lift forces.

5. Evaluation of the virtual force term

So as to demonstrate the effectiveness of the virtual force term, the latter is evaluated approximately in this section for two distinct cases: solid–liquid two-phase flow with spherical solid particles in creeping flow; and gas–liquid two-phase flow with large bubbles in highly turbulent flow. Denote the virtual force term by $\boldsymbol{F}_v$. The exact expression for $\boldsymbol{F}_v$ is the second term on the right-hand side of (3.19):

$$\boldsymbol{F}_v = \frac{1}{\Lambda}\int_0^{\pi}\mathrm{d}\theta\int_0^{2\pi}\mathrm{d}\phi\,[R^3\sin\theta\,\{\boldsymbol{n}(\theta,\phi)\cdot(\nabla\lambda_R)|_{X_0}\}\times\boldsymbol{n}(\theta,\phi)\cdot\Delta\overline{\boldsymbol{T}_c}^{\Lambda}(\boldsymbol{X}_0:R,\theta,\phi)]. \quad (5.1)$$

Equation (5.1) can be generalized for non-spherical particles, as described in Appendix D of the supplementary material, to

$$\boldsymbol{F}_v = \frac{1}{\Lambda}\int_0^{\pi}\mathrm{d}\theta\int_0^{2\pi}\mathrm{d}\phi\,[R(\theta,\phi)^3C(\theta,\phi)\sin\theta\,\{\boldsymbol{i}_r(\theta,\phi)\cdot(\nabla\lambda_R)|_{X_0}\}\times\boldsymbol{n}(\boldsymbol{X}_0:R(\theta,\phi),\theta,\phi)\cdot\Delta\overline{\boldsymbol{T}_c}^{\Lambda}(\boldsymbol{X}_0:R(\theta,\phi),\theta,\phi)]. \quad (5.2)$$

https://doi.org/10.1017/jfm.2011.452 Published online by Cambridge University Press

5.1. *Spherical solid particles in creeping flow*

The spatial distributions of velocity and static pressure surrounding a rigid sphere for creeping flow are given by (Bird, Stewart & Lightfoot 1962):

$$P_c = P_0 - \rho_c g Z - \frac{3}{2}\frac{\mu_c v_\infty}{R}\left(\frac{R}{r}\right)^2 \cos\theta, \tag{5.3}$$

$$v_r = v_\infty \left\{1 - \frac{3}{2}\left(\frac{R}{r}\right) + \frac{1}{2}\left(\frac{R}{r}\right)^3\right\} \cos\theta, \tag{5.4}$$

$$v_\theta = -v_\infty \left\{1 - \frac{3}{4}\left(\frac{R}{r}\right) - \frac{1}{4}\left(\frac{R}{r}\right)^3\right\} \sin\theta. \tag{5.5}$$

Here, R is the radius of the spherical particle, ρ_c and μ_c are the density and viscosity of the surrounding fluid, the Z axis is directed upwards with its origin at the centre of the sphere, P_0 is the static pressure of outer flow at $Z = 0$, and a spherical coordinate system is used with its origin at the centre of the particle. The angular coordinate θ is defined with respect to the Z axis, and the velocity field at infinite distance from the sphere is $-\boldsymbol{i}_Z v_\infty$. The flow field surrounding a particle in the dispersed solid–liquid two-phase flow is different from that for a particle in the liquid phase even for a case of creeping flow. However, let us assume that the flow field given by (5.3), (5.4) and (5.5) can be utilized for the dispersed solid–liquid two-phase flow, to see the effectiveness of the virtual force term. Since the azimuthal component and gradient of the velocity are zero for irrotational creeping flow, the shear stress tensor of the flow is obtained as

$$\begin{aligned}\boldsymbol{\tau}_c = {} & \boldsymbol{i}_r\boldsymbol{i}_r\mu\left(-2\frac{\partial v_r}{\partial r}\right) + \boldsymbol{i}_\theta\boldsymbol{i}_\theta\mu\left\{-2\left(\frac{1}{r}\frac{\partial v_\theta}{\partial\theta} + \frac{v_r}{r}\right)\right\} + \boldsymbol{i}_\phi\boldsymbol{i}_\phi\mu\left\{-2\left(\frac{v_r}{r} + \frac{v_\theta\cot\theta}{r}\right)\right\} \\ & + (\boldsymbol{i}_r\boldsymbol{i}_\theta + \boldsymbol{i}_\theta\boldsymbol{i}_r)\mu\left[-\left\{r\frac{\partial}{\partial r}\left(\frac{v_\theta}{r}\right) + \frac{1}{r}\frac{\partial v_r}{\partial\theta}\right\}\right].\end{aligned} \tag{5.6}$$

Next, $\Delta\boldsymbol{T}_c$ for the irrotational creeping flow is given by

$$(\Delta\boldsymbol{T}_c)|_{r=R} = \frac{3}{2}\frac{\mu v_\infty}{R}\{(\boldsymbol{i}_r\boldsymbol{i}_\theta + \boldsymbol{i}_\theta\boldsymbol{i}_r)\sin\theta - \boldsymbol{I}\cos\theta\}. \tag{5.7}$$

Let us express the gradient of the local holdup as:

$$(\nabla\lambda_R)|_{X_0} = a_X\boldsymbol{i}_X + a_Y\boldsymbol{i}_Y + a_Z\boldsymbol{i}_Z. \tag{5.8}$$

Then, the virtual force term for the creeping flow is

$$\begin{aligned}\boldsymbol{F}_v &= \frac{1}{\Lambda}\frac{3}{2}\frac{\mu_c v_\infty}{R}\int_0^\pi \mathrm{d}\theta\int_0^{2\pi}\mathrm{d}\phi\,[R^3\sin\theta\,(\boldsymbol{i}_\theta\sin\theta - \boldsymbol{i}_r\cos\theta)\{\boldsymbol{n}(\theta,\phi)\cdot(\nabla\lambda_R)|_{X_0}\}] \\ &= -\boldsymbol{i}_Z\frac{1}{\Lambda}\frac{3}{2}(\mu_c v_\infty R^2)\int_0^\pi \mathrm{d}\theta\int_0^{2\pi}\mathrm{d}\phi\,[\sin\theta\,(a_X\sin\theta\cos\phi + a_Y\sin\theta\sin\phi + a_Z\cos\theta)] \\ &= 0.\end{aligned} \tag{5.9}$$

The relations $\boldsymbol{n}(\theta,\phi)\cdot(\nabla\lambda_R)|_{X_0} = a_X\sin\theta\cos\phi + a_Y\sin\theta\sin\phi + a_Z\cos\theta$, $\boldsymbol{i}_r = \boldsymbol{i}_X\sin\theta\cos\phi + \boldsymbol{i}_Y\sin\theta\sin\phi + \boldsymbol{i}_Z\cos\theta$ and $\boldsymbol{i}_\theta = \boldsymbol{i}_X\cos\theta\cos\phi + \boldsymbol{i}_Y\cos\theta\sin\phi - \boldsymbol{i}_Z\sin\theta$ have been used. The virtual force term vanishes for irrotational creeping flow with uniform size of the solid spheres. This result does not contradict the finding by Ten Cate & Sundaresan (2006), using numerical simulation based on the lattice–Boltzmann

https://doi.org/10.1017/jfm.2011.452 Published online by Cambridge University Press

method, that the term involving the spatial gradient of the local holdup does not influence homogeneous flow through a particle-packed bed with a spatial gradient of packing. Although the Reynolds number in Cate and Sundaresan's numerical experiments is about 10 times larger than that for creeping flow, the contribution of the Reynolds stress still appears to be small.

Consider now the effect of taking different values of v_∞ for hemispheres with positive and negative values of Y, and consider a case in which the velocity vector $\overline{\boldsymbol{u}_c}^c$ is not homogeneous, but varies along the Y axis. In that case,

$$\begin{aligned}\boldsymbol{F}_v &= -\boldsymbol{i}_Z \frac{1}{\Lambda}\frac{3}{2}(\mu v_\infty^+ R^2)\int_0^\pi \mathrm{d}\theta \int_0^\pi \mathrm{d}\phi\,[\sin\theta\,(a_X \sin\theta\cos\phi + a_Y \sin\theta\sin\phi + a_Z\cos\theta)] \\ &\quad -\boldsymbol{i}_Z \frac{1}{\Lambda}\frac{3}{2}(\mu v_\infty^- R^2)\int_0^\pi \mathrm{d}\theta \int_\pi^{2\pi} \mathrm{d}\phi\,[\sin\theta\,(a_X \sin\theta\cos\phi + a_Y \sin\theta\sin\phi + a_Z\cos\theta)] \\ &= -\boldsymbol{i}_Z \frac{3a_Y\pi}{2\Lambda}(\mu_c R^2)(v_\infty^+ - v_\infty^-) \approx -\boldsymbol{i}_Z \frac{9}{8R}\left(\frac{\partial\epsilon}{\partial Y}\right)\bigg|_{X_0} \mu_c(v_\infty^+ - v_\infty^-). \end{aligned} \tag{5.10}$$

Here, the relation $(a_Y/\Lambda)(4\pi R^3/3) \approx (\partial\epsilon/\partial Y)|_{X_0}$ has been used. The symbols v_∞^+ and v_∞^- denote velocities representative of regions with positive and negative value of Y axis, respectively. Equation (5.10) shows that the virtual force term has a non-zero component along the flow direction in the case where the gradient of the local holdup is not perpendicular to the velocity gradient. The Stokes drag term in the two-fluid model equation is given by $\epsilon 6\pi R^2 \mu_c v_\infty (3/4\pi R^3)$, so that the ratio of the last term in (5.10) to the Stokes drag term is $(1/4R\epsilon)(\partial\epsilon/\partial Y)|_{X_0}(v_\infty^+ - v_\infty^-)/v_\infty$. The values of $(1/R\epsilon)(\partial\epsilon/\partial Y)|_{X_0}$ and $(v_\infty^+ - v_\infty^-)/v_\infty$ should vary case by case, but the value of the virtual force term seems to be considerably smaller than the Stokes drag term.

Theoretical and/or experimental studies on the distribution of $\Delta\overline{\boldsymbol{T}_c^\Lambda}$ on a particle surface for individual cases should provide reliable values of the virtual force term.

5.2. *Gas–liquid dispersed flow with spherical cap bubbles*

It is well known that the shape of a rising bubble depends on its size and on the flow field surrounding the bubble. The bubble changes from spherical to ellipsoidal in shape, and finally becomes a spherical cap bubble with increase in its size (Tadaki & Maeda 1961); the shape may be skewed when the bubble rises in a flow with a lateral velocity gradient, where the bubble laterally migrates, as experimentally confirmed by Tomiyama *et al.* (2002). In this section the virtual force term is evaluated for gas–liquid dispersed flow in bubble columns in a recirculating turbulent flow regime, the bubble size for which is known to be in the category of spherical cap bubble (Ueyama & Miyauchi 1979).

Tadaki & Maeda (1961) found experimentally that the rising velocity of a spherical cap bubble depends solely on bubble size as

$$u_b = 0.716\sqrt{d_e g}, \tag{5.11}$$

where d_e is the sphere equivalent diameter of the bubble, and g is the gravitational acceleration. They specified the shape of spherical cap bubbles as shown in figure 4, and relations $d_e = 0.62a$ and $R_s = 0.933d_e$ were confirmed experimentally, where a is the horizontal diameter of the bubble and R_s is the radius of the topmost spherical surface. Davies & Taylor (1950) obtained theoretically an equation almost identical to (5.11) on the basis of potential flow in the vicinity of the stagnation point at the top of a bubble. Joseph (2003) developed a theory based on the viscous potential flow in the

https://doi.org/10.1017/jfm.2011.452 Published online by Cambridge University Press

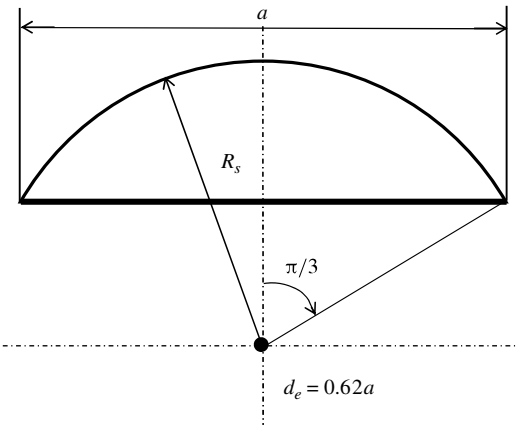


FIGURE 4. Spherical cap bubble.

vicinity of the stagnation point at the top of the bubble so as to incorporate the effect of viscosity,

$$u_b = -\frac{4}{3}\frac{\nu}{R_s} + \sqrt{\frac{4}{9}R_s g + \left(\frac{\nu}{R_s}\right)^2}, \tag{5.12}$$

where ν is the kinematic viscosity of the liquid. Since the radius of the spherical surface of the spherical cap bubble is greater than 1 cm, (5.12) gives almost the same terminal velocity as (5.11).

The left-hand sides of (4.1) and (4.3) are zero for the terminal velocity:

$$0 = -\oint_{S_p} \boldsymbol{n} P_c \,\mathrm{d}S - \oint_{S_p} \boldsymbol{n}\cdot\boldsymbol{\tau}_c \,\mathrm{d}S + \boldsymbol{g}\int_{V_p} \rho_p \,\mathrm{d}V, \tag{5.13}$$

$$0 = -\oint_{S_p} \boldsymbol{n}\Delta P_c \,\mathrm{d}S - \oint_{S_p} \boldsymbol{n}\cdot\Delta\boldsymbol{\tau}_c \,\mathrm{d}S + \boldsymbol{g}\int_{V_p} (\rho_p - \rho_c) \,\mathrm{d}V. \tag{5.14}$$

The terminal velocity given by (5.11) is independent of viscosity, so that the second terms on the right-hand sides of (5.13) and (5.14) are negligible compared to the first and third terms in the equations:

$$0 \approx -\oint_{S_p} \boldsymbol{n} P_c \,\mathrm{d}S + \boldsymbol{g}\int_{V_p} \rho_p \,\mathrm{d}V, \tag{5.15}$$

$$0 \approx -\oint_{S_p} \boldsymbol{n}\Delta P_c \,\mathrm{d}S + \boldsymbol{g}\int_{V_p} (\rho_p - \rho_c) \,\mathrm{d}V. \tag{5.16}$$

Equations (5.15) and (5.16) resemble each other, but their physical meanings should be distinguished. Considering that the density of the gas phase is very small, (5.15) means that the contribution of the excess pressure on the bubble surface, $-\oint_{S_p} \boldsymbol{n}\Delta P_c$, almost compensates the contribution of total static pressure on the surface of the conceptual sphere, $-\oint_{S_p} \boldsymbol{n} P_c^b$. Equation (5.16) shows that the contribution of the excess pressure is in a balance with the buoyancy acting on the particle, the magnitude of which is around 1000 times larger than the terms in (5.15). The balance seems to be the essential mechanism determining the rising velocity of a spherical cap bubble

https://doi.org/10.1017/jfm.2011.452 Published online by Cambridge University Press

as a function of bubble size and gravitational acceleration, independently of liquid viscosity.

For a spherical cap bubble in a stationary dispersed gas–liquid multiphase flow, (4.12) can be applied, to give

$$0 \approx -\oint_{S_p} \boldsymbol{n} \cdot \overline{\boldsymbol{\tau}_R}^c \, \mathrm{d}S - \oint_{S_p} \boldsymbol{n} \cdot \Delta \overline{\boldsymbol{T}_c^A} \, \mathrm{d}S + \boldsymbol{g} \int_{V_p} (\rho_p - \rho_m) \, \mathrm{d}V. \tag{5.17}$$

In bubble columns operating in a recirculating turbulent flow regime, it is well known that large bubbles in a category of spherical cap bubbles rise with relative velocity given by (5.11) (Ueyama & Miyauchi 1979). The principal mechanism controlling the rising velocity of the large bubbles in a highly turbulent dispersed gas–liquid flow should therefore be similar to that in a stationary flow of liquid. The Reynolds stress term $\overline{\boldsymbol{\tau}_R}^c$ for the recirculating turbulent flow in bubble columns has been treated theoretically so as to fit the experimental data for the radial distributions of the time-averaged velocity of the liquid phase and the gas holdup (Ueyama & Miyauchi 1979). Based on their analysis, the value of $\boldsymbol{\nabla} \cdot \overline{\boldsymbol{\tau}_R}^c$ can be calculated as

$$\boldsymbol{\nabla} \cdot \overline{\boldsymbol{\tau}_R}^c = -\frac{\rho_c \nu_t}{\gamma} \frac{\partial}{\partial \gamma} \left(\gamma \frac{\partial \overline{u_z}^c}{\partial \gamma} \right) = \rho_c \nu_t \frac{8(\overline{u_z}^c|_{\gamma=0} - \overline{u_z}^c|_{\gamma=\Gamma})}{\Gamma^2} \left\{ 1 - 2\left(\frac{\gamma}{\Gamma} \right)^2 \right\}. \tag{5.18}$$

Here, the right-hand side is specified in cylindrical coordinates with z and γ as axial and radial coordinates; Γ is the column radius. The symbols $\overline{u_z}^c|_{\gamma=0}$ and $\overline{u_z}^c|_{\gamma=\Gamma}$ denote the time-averaged axial velocity component of $\boldsymbol{u}_c$ at the centre of the column and just outside the boundary layer on the column wall. Also, ν_t denotes the kinematic turbulent viscosity, which has been found experimentally to be $\nu_t = 0.0322\,(2\Gamma)^{1.70}$, where the values of ν_t and Γ are in SI units (Miyauchi *et al.* 1981). By introducing experimental data for $\Gamma = 0.30$ m and with a superficial gas velocity of 0.6 m s^{-1}, the value of $\boldsymbol{\nabla} \cdot \overline{\boldsymbol{\tau}_R}^c$ increases monotonically from -2300 kg m^{-2} s^{-2} at the centre of the column to $+2300$ kg m^{-2} s^{-2} at the column wall. The value of $\boldsymbol{g}(\rho_p - \rho_m)$ under the same experimental conditions is approximately 6000 kg m^{-2} s^{-2} throughout the entire region of the column. It can be concluded that the first term on the right-hand side of (5.17) is considerably smaller in magnitude relative to the third term. In most of the column, we have

$$0 \approx -\oint_{S_p} \boldsymbol{n} \Delta \overline{P_c^A} \, \mathrm{d}S + \boldsymbol{g} \int_{V_p} (\rho_p - \rho_m) \, \mathrm{d}V. \tag{5.19}$$

In deriving this relation, a term $\oint_{S_p} \boldsymbol{n} \cdot \Delta \overline{\boldsymbol{\tau}_c^A} \, \mathrm{d}S$ has been neglected relative to $\oint_{S_p} \boldsymbol{n} \cdot \overline{\boldsymbol{\tau}_R}^c \, \mathrm{d}S$. Equation (5.19) indicates that, once again, the rising velocity of a spherical cap bubble in gas–liquid dispersed two-phase flow is determined by the balance between the contribution of the excess pressure ΔP_c on the bubble surface and the buoyancy term. This explains why the rising velocity of bubbles relative to the liquid flow measured in a bubble column operating in the recirculating turbulent flow regime coincides with the value calculated from (5.11).

By using Gauss' theorem, (5.19) is transformed to

$$\oint_{S_p} \boldsymbol{n} \Delta \overline{P_c^A} \, \mathrm{d}S \approx \oint_{S_p} \boldsymbol{n} (\rho_m - \rho_p) g Z \, \mathrm{d}S. \tag{5.20}$$

Here, the Z axis is chosen to be opposite to the direction of gravitational acceleration. Equation (5.20) does not assure equality between $\boldsymbol{n} \Delta \overline{P_c^A}$ and $\boldsymbol{n}(\rho_m - \rho_p) g Z$ at every

https://doi.org/10.1017/jfm.2011.452 Published online by Cambridge University Press

point, however. Let us see what happens upon exchanging $\boldsymbol{n}\Delta\overline{P_c^{\Lambda}}$ with $\boldsymbol{n}(\rho_m-\rho_p)gZ$ in the calculation of the virtual force term, and so deduce how the virtual force term acts in the case of dispersed gas–liquid multiphase flow with spherical cap bubbles.

Although the shape of the bubbles in bubble columns operated in the recirculating turbulent flow regime is considerably deformed due to turbulence, we assume that the mean shape of the bubbles is a spherical cap as shown in figure 4, owing to the experimental finding that the bubble rising velocity coincides with the rising velocity of the spherical cap bubble given by (5.11). From (5.2), the virtual force term for the dispersed gas–liquid multiphase flow with spherical cap bubbles is given by

$$\begin{aligned}\boldsymbol{F}_v=&\frac{1}{\Lambda}\int_0^{\pi/3}\mathrm{d}\theta\int_0^{2\pi}\mathrm{d}\phi\,[(R_s)^3\sin\theta\,\{\boldsymbol{i}_r(\theta,\phi)\cdot(\nabla\lambda_R)|_{X_0}\}\\&\times\boldsymbol{n}(\boldsymbol{X}_0:R_s,\theta,\phi)\Delta\overline{P_c^{\Lambda}}(\boldsymbol{X}_0:R_s,\theta,\phi)]\\&+\frac{1}{\Lambda}\int_0^{\pi/3}\mathrm{d}\theta\int_0^{2\pi}\mathrm{d}\phi\,[(r_B)^3\tan\theta\,\{\boldsymbol{i}_r(\theta,\phi)\cdot(\nabla\lambda_R)|_{X_0}\}\\&\times(-\boldsymbol{i}_Z)\Delta\overline{P_c^{\Lambda}}(\boldsymbol{X}_0:r_B,\theta,\phi)].\end{aligned}\tag{5.21}$$

The first and second terms on the right-hand side correspond, respectively, to the top spherical surface and the bottom flat surface. The symbol $r_B=(R_s/\cos\theta)\cos(\pi/3)=R_s/(2\cos\theta)$ refers to the r coordinate of the bottom surface in a spherical coordinate system $(\boldsymbol{X}_0:r,\theta,\phi)$, the origin of which is set at the centre of the top spherical surface. By exchanging $\boldsymbol{n}\Delta\overline{P_c^{\Lambda}}$ with $\boldsymbol{n}(\rho_m-\rho_p)gZ$, we can proceed with the calculation of the right-hand side of (5.21). The X, Y and Z components of the virtual force term are calculated as

$$\begin{aligned}\boldsymbol{i}_X\cdot\boldsymbol{F}_v=&\frac{1}{\Lambda}(\rho_m-\rho_p)gR_s^4\int_0^{\pi/3}\mathrm{d}\theta\int_0^{2\pi}\mathrm{d}\phi\,[a_X\sin^3\theta\cos\theta\cos^2\phi\\&+a_Y\sin^3\theta\cos\theta\sin\phi\cos\phi+a_Z\sin^2\theta\cos^2\theta\cos\phi]\\=&\frac{9}{64}\pi\frac{a_X}{\Lambda}(\rho_m-\rho_p)gR_s^4\approx0.686(\rho_m-\rho_p)gR_s\left(\frac{\partial\epsilon}{\partial X}\right)\Big|_{X_0},\end{aligned}\tag{5.22}$$

$$\begin{aligned}\boldsymbol{i}_Y\cdot\boldsymbol{F}_v=&\frac{1}{\Lambda}(\rho_m-\rho_p)gR_s^4\int_0^{\pi/3}\mathrm{d}\theta\int_0^{2\pi}\mathrm{d}\phi\,[a_X\sin^3\theta\cos\theta\sin\phi\cos\phi\\&+a_Y\sin^3\theta\cos\theta\sin^2\phi+a_Z\sin^2\theta\cos^2\theta\sin\phi]\\=&\frac{9}{64}\pi\frac{a_Y}{\Lambda}(\rho_m-\rho_p)gR_s^4\approx0.686(\rho_m-\rho_p)gR_s\left(\frac{\partial\epsilon}{\partial Y}\right)\Big|_{X_0},\end{aligned}\tag{5.23}$$

$$\begin{aligned}\boldsymbol{i}_Z\cdot\boldsymbol{F}_v=&\frac{1}{\Lambda}(\rho_m-\rho_p)gR_s^4\int_0^{\pi/3}\mathrm{d}\theta\int_0^{2\pi}\mathrm{d}\phi\,[a_X\sin^2\theta\cos^2\theta\cos\phi\\&+a_Y\sin^2\theta\cos^2\theta\sin\phi+a_Z\sin\theta\cos^3\theta]\\&-\frac{1}{\Lambda}(\rho_m-\rho_p)g\frac{R_s^4}{16}\int_0^{\pi/3}\mathrm{d}\theta\int_0^{2\pi}\mathrm{d}\phi\\&\times\left[\frac{\tan\theta}{\cos^3\theta}(a_X\sin\theta\cos\phi+a_Y\sin\theta\sin\phi+a_Z\cos\theta)\right]\\=&\frac{9}{32}\pi\frac{a_Z}{\Lambda}(\rho_m-\rho_p)gR_s^4\approx1.37(\rho_m-\rho_p)gR_s\left(\frac{\partial\epsilon}{\partial Z}\right)\Big|_{X_0}.\end{aligned}\tag{5.24}$$

https://doi.org/10.1017/jfm.2011.452 Published online by Cambridge University Press

Here, (5.8) has been used, together with the relations $V_p(\lambda_R)|_{X_0} \approx \Lambda(\epsilon)|_{X_0}$, $Z = R_s \cos\theta$, $V_p = (\pi/6)d_e^3 = 0.205\pi R_s^3$, $\int_0^{\pi/3} \sin^3\theta \cos\theta \, \mathrm{d}\theta = 9/64$, $\int_0^{2\pi} \cos^2\phi \, \mathrm{d}\phi = \int_0^{2\pi} \sin^2\phi \, \mathrm{d}\phi = \pi$ and $\int_0^{\pi/3} (\tan\theta/\cos^2\theta) \, \mathrm{d}\theta = 3/2$. For gas–liquid dispersed multiphase flow in bubble columns operating in the recirculating turbulent flow regime, the local holdup of the gas phase is vertically homogeneous and horizontally distributed. For the equation of motion of a spherical cap bubble in dispersed gas–liquid multiphase flow, considered by Ueyama & Miyauchi (1979), with a column diameter of 0.6 m and superficial gas velocity 0.6 m s^{-1}, the radial component of the virtual force term is approximately

$$\begin{aligned} & 0.686(\rho_m - \rho_p) g R_s \left(\frac{\partial \epsilon}{\partial \gamma} \right) \Bigg|_{X_0} \boldsymbol{i}_\gamma \\ & \quad \approx 0.686(0.6 \times 10^3 \text{ kg m}^{-3})(9.8 \text{ m s}^{-2})(0.02 \text{ m}) \left(-\frac{0.4}{0.3} \text{ m} \right) \boldsymbol{i}_\gamma \\ & \quad \approx -\boldsymbol{i}_\gamma \times 108 \text{ kg m}^{-2} \text{ s}^{-2}. \end{aligned} \tag{5.25}$$

Tomiyama *et al.* (2002) determined experimentally the value of the transverse lift coefficient for large bubbles to be $C_{TL} \approx -0.3$. The lateral component of the conventional interaction term is then

$$\begin{aligned} & -\epsilon \{ C_{TL} \rho_c (\overline{\boldsymbol{u}_p^{\Lambda}} - \overline{\boldsymbol{u}_p}^c) \times \nabla \times \overline{\boldsymbol{u}_p}^c \} \\ & \quad \approx -\epsilon \left\{ C_{TL} \rho_c (\overline{\boldsymbol{u}_p^{\Lambda}} - \overline{\boldsymbol{u}_p}^c) \times \boldsymbol{i}_\theta \left(-\frac{\partial \overline{u_{c,z}}^c}{\partial \gamma} \right) \right\} \\ & \quad \approx -0.4 \left\{ -0.3 \times 10^3 \text{ kg m}^{-3} (\boldsymbol{i}_Z \times 0.3 \text{ m s}^{-1}) \times \boldsymbol{i}_\theta \left(\frac{2 \text{ m s}^{-1}}{0.3 \text{ m}} \right) \right\} \\ & \quad \approx -\boldsymbol{i}_\gamma \times 240 \text{ kg m}^{-2} \text{ s}^{-2}. \end{aligned} \tag{5.26}$$

We know that the numerical value of the virtual force term is almost half of the lift force term with the same sign in the case of dispersed gas–liquid two-phase flow in bubble columns operating in a recirculating turbulent flow regime. Since the virtual force term appears only in the two-fluid model equation, the preceding discussion does not affect the previous treatment of the equation of motion for a particle. The virtual force term, however, should be significant in the two-fluid model equation for the liquid phase in dispersed gas–liquid flow in bubble columns. This term will be important in the mechanism controlling the horizontal distribution of macroscopic properties such as the averaged liquid velocity and the local holdup of the bubble phase. Although equality between $\boldsymbol{n}\Delta\overline{P_c^{\Lambda}}$ and $\boldsymbol{n}(\rho_m - \rho_p)gZ$ at every point has been assumed in the calculation, the virtual force term appears to influence numerical results based on the two-fluid model equation.

Theoretical and experimental studies on the distribution of $\boldsymbol{n} \cdot (\Delta\overline{P_c^{\Lambda}}\boldsymbol{I} + \Delta\overline{\boldsymbol{\tau}_c^{\Lambda}})$ on the particle surface for various cases are urgent for reliable estimation of the virtual mass force.

6. Two-fluid model equations

By substituting (3.20) into (2.13), we have

$$\begin{aligned} & \frac{\partial}{\partial t} \{ (1-\epsilon) \overline{\rho_c \boldsymbol{u}_c}^c \} + \nabla \cdot \{ (1-\epsilon) \overline{\rho_c \boldsymbol{u}_c \boldsymbol{u}_c}^c \} \\ & \quad = -\epsilon \frac{\overline{\boldsymbol{f}_p^{\Delta\tau}}}{V_p} - (1-\epsilon)(\nabla \overline{P_c}^c) - (1-\epsilon)(\nabla \cdot \overline{\boldsymbol{\tau}_c}^c) + (1-\epsilon)\overline{\rho_c}^c \boldsymbol{g} - \boldsymbol{F}_v. \end{aligned} \tag{6.1}$$

https://doi.org/10.1017/jfm.2011.452 Published online by Cambridge University Press

Equation (6.1) is the two-fluid model equation for the continuous phase, without any restriction on averaging.

The first, second and fourth terms on the right-hand side are also found in the conventional two-fluid model equation.

The third term, $-(1-\epsilon)(\nabla\cdot\overline{\boldsymbol{\tau}_c}^c)$, is slightly different from that in the conventional two-fluid model equation, $-\nabla\cdot\{(1-\epsilon)\overline{\boldsymbol{\tau}_c}^c\}$. This is because we have taken $\Delta\overline{\boldsymbol{T}_c^A}$ to define the force acting on a drop, $\overline{\boldsymbol{f}_p^{\Delta T}}$, according to (3.10). In deriving the two-fluid model equation via volume averaging, the contribution of the shear stress tensor $\boldsymbol{\tau}_c$ is omitted from the argument, although the difference between shear stress tensors on a drop surface and in the bulk of the continuous phase has also been noted (Kolev 2007).

The fifth term on the right-hand side of (6.1), $\boldsymbol{F}_v$, is proposed here as the virtual force term, which reflects the 'inside-out' property of the interaction term. The value of $\boldsymbol{F}_v$ can be calculated by introducing the local gradient of the holdup and distributions of pressure and shear stress on a particle surface into (3.21). The main property of the term is proportional to $\nabla\epsilon$, as seen in (3.22), and is finally approximated to a product of the local gradient of the holdup and the difference between the forces acting on hemispherical surfaces of the drop divided by a plane perpendicular to the gradient vector $\nabla\epsilon$, that is, $-cR(\partial\epsilon/\partial Z)|_{\boldsymbol{X}_0}(\overline{\boldsymbol{f}_p^{\Delta T+}}(\boldsymbol{X}_0)-\overline{\boldsymbol{f}_p^{\Delta T-}}(\boldsymbol{X}_0))/V_p$. The term proportional to $\nabla\epsilon$ becomes significant in simulating the macroscopic property of spatially inhomogeneous multiphase flow, like the dispersion force introduced for physical reasons (Lahey *et al.* 1993; de Bertodano *et al.* 1994; Zhang & Prosperetti 1994), which has been the only term with $\nabla\epsilon$ in the conventional two-fluid model equation.

The Reynolds stress term emerges from the second term on the left-hand side of (6.1). This work does not investigate in detail of the Reynolds stress term for the dispersed multiphase flow.

7. Conclusion

Equation (2.13) has been obtained as the two-fluid model equation without any restriction on averaging, and the physical meaning of the interaction term was shown to be the limiting value for infinitesimal control volume of the time-averaged force acting on particle surfaces in a control volume.

The interaction term in the two-fluid model equation has been determined for dispersed two-phase flow with homogeneous particle size, and differs from the conventional interaction term in its 'inside-out' property, seen in (3.8).

The 'inside-out' interaction term given by (3.8) has been shown to be identical with the impulse term, given as the interaction term in the two-fluid model equation based on time averaging.

The 'inside-out' interaction term was then transformed to the conventional interaction term and the virtual force term $\boldsymbol{F}_v$ by using a Taylor expansion to shift the point at which the physical quantities are assigned and truncating this expansion. The virtual force term is given as (3.21), the value of which can be calculated by using a spatial distribution of the local holdup and distributions of pressure and shear stress on a particle surface centred at the point of interest.

The equation of motion for a particle in the dispersed two-phase flow has been discussed, using the time-averaged moving velocity of a particle precisely defined in Appendix G of the supplementary material. A relation between the time-averaged moving velocity of a particle and the time-averaged velocity of the dispersed phase

https://doi.org/10.1017/jfm.2011.452 Published online by Cambridge University Press

has been derived, which shows that the two averaged velocities are to be distinguished when neither the time-averaged moving velocity of particles nor the local holdup are homogeneous in space. The buoyancy term has been picked out of the equation of motion for a particle by using the relevant Navier–Stokes equation, and the reference density in the buoyancy term has been shown to be the mean density of the surrounding two-phase mixture. The physical meanings of the terms in the equation of motion were assigned.

The virtual force term was evaluated approximately in two cases, in order to demonstrate how this term acts. For spherical solid particles in creeping flow, the virtual force term vanished for a homogeneous flow field, as was found numerically by Ten Cate & Sundaresan (2006). It was also shown, however, that the virtual force term may make a significant contribution when the flow field has a velocity gradient that is not perpendicular to the gradient of the local holdup of the particle phase. For spherical cap bubbles in highly turbulent gas–liquid multiphase flow in bubble columns, the virtual force term was shown to influence the lateral distribution of macroscopic properties of the gas–liquid multiphase flow.

The corrected two-fluid model equation was derived as (6.1), which includes a new term $\boldsymbol{F}_v$, that is, the virtual force term. Theoretical and experimental studies of the consequences of this term are urged.

It should be noted here that the expression of the virtual force term, $\boldsymbol{F}_v$, is different from (3.21) in the wall region within a distance equal to the particle diameter from the wall, because part of the spherical surface illustrated in figure 3 cannot be occupied by a particle centre when the point of interest is in the wall region. A model for the virtual force term in the wall region will soon be submitted, together with a discussion on the boundary conditions for the equation of motion for a particle and the two-fluid model equations for the continuous and dispersed phases.

Acknowledgements

The author is grateful to Dr Hiroshi Takeda of the R-Flow Company for valuable discussions about two-fluid model equations, and for asking pertinent questions.

The appendices are available as supplementary material at journals.cambridge.org/flm.

REFERENCES

ANDERSON, T. B. & JACKSON, R. 1967 A fluid mechanical description of fluidized beds. *Ind. Engng Chem. Fundam.* **6**, 527–539.

BATCHELOR, G. K. 1970 The stress system in a suspension of force-free particles. *J. Fluid Mech.* **41** (3), 545–570.

DE BERTODANO, M. L., LAHEY, R. T. JR. & JONES, O. C. 1994 Phase distribution in bubbly two-phase flow in vertical ducts. *Intl J. Multiphase Flow* **20**, 805–818.

BIRD, R. B., STEWART, W. E. & LIGHTFOOT, E. N. 1962 *Transport Phenomena*, 2nd edn. John Wiley & Sons.

BRENNEN, C. E. 2005 *Fundamentals of Multiphase Flow*. Cambridge University Press.

DAVIES, R. M. & TAYLOR, G. I. 1950 The mechanics of large bubbles rising through extended liquids and through liquids in tubes. *Proc. R. Soc. Lond.* A **20**, 375–390.

DREW, D. A. 1983 Mathematical modelling of two-phase flow. *Annu. Rev. Fluid Mech.* **15**, 261–291.

HIBIKI, T. & ISHII, M. 2007 Lift force in bubbly flow systems. *Chem. Engng. Sci.* **62**, 6457–6474.

HINCH, E. J. 1977 An averaged-equation approach to particle interaction in a fluid suspension. *J. Fluid Mech.* **83** (4), 695–720.

https://doi.org/10.1017/jfm.2011.452 Published online by Cambridge University Press

ISHII, M. 1975 *Thermo-Fluid Dynamics Theory of Two-Phase Flow*. *Collection de la Direction des Études et Recherches d'Electricité de France*, Eyrolles.

ISHII, M. & HIBIKI, T. 2006 *Thermo-Fluid Dynamics of Two-Phase Flow*. Springer.

JACKSON, R 2000 *The Dynamics of Fluidized Particles*. Cambridge University Press.

JOSEPH, D. D. 2003 Rise velocity of a spherical cap bubble. *J. Fluid Mech.* **488**, 213–223.

KOLEV, N. I. 2007 *Multiphase Flow Dynamics*, 3rd edn. Springer.

KULKARNI, A. A. 2008 Lift force on bubbles in a bubble column reactor: experimental analysis. *Chem. Engng Sci.* **63**, 1710–1723.

LAHEY, R. T. JR, BERTODANO, M. L. & JONES, O. C. 1993 Phase distribution in complex geometry conduits. *Nucl. Engng Des.* **141**, 177–201.

MIYAUCHI, T., FURUSAKI, S., MOROOKA, S. & IKEDA, Y. 1981 Transport phenomena and reaction in fluidized catalyst beds. *Adv. Chem. Engng* **11**, 275–448.

SLATTERY, J. C. 1967 Flow of viscoelastic fluids through porous media. *AIChE J.* **13**, 1066–1071.

TABIB, M. V., ROY, S. A. & JOSHI, J. B. 2008 CFD simulation of bubble column – An analysis of interphase forces and turbulence models. *Chem. Engng J.* **139**, 589–614.

TADAKI, T. & MAEDA, S. 1961 On the shape and velocity of single air bubble rising in various liquids. *Kagakukogaku* **25**, 254–264.

TEN CATE, A. & SUNDARESAN, S. 2006 Analysis of the flow in inhomogeneous particle beds using the spatially averaged two-fluid equations. *Intl J. Multiphase Flow* **32**, 106–131.

TOMIYAMA, A., TAMAI, H., ZUN, I. & HOSOKAWA, S. 2002 Transverse migration of single bubbles in simple shear flows. *Chem. Engng Sci.* **57**, 1849–1858.

UEYAMA, K. & MIYAUCHI, T. 1976 Time-averaged Navier–Stokes equations as basic equations for multiphase flow. *Kagakukogaku Ronbunsyu* **2**, 595–601.

UEYAMA, K. & MIYAUCHI, T. 1979 Properties of recirculating turbulent two phase flow in bubble columns. *AIChE J.* **25**, 258–266.

WHITAKER, S. 1967 Diffusion and dispersion in porous media. *AIChE J.* **13**, 420–427.

ZHANG, D., DEEN, N. D. & KUIPERS, J. A. M. 2006 Numerical simulation of the dynamic flow behaviour in a bubble column: a study of closures for turbulence and interface forces. *Chem. Engng Sci.* **61**, 7593–7608.

ZHANG, D. Z. & PROSPERETTI, A. 1994 Averaged equations for inviscid disperse two-phase flow. *J. Fluid Mech.* **267**, 185–219.

https://doi.org/10.1017/jfm.2011.452 Published online by Cambridge University Press